Pannaree Boonyuen, Girton College

Rice Tungro Disease: The Effect of transmission rates on the disease dynamics and the cost-effectiveness of different roguing patterns

Nik Cunniffe, Rachel Murray-Watson

Word count: 5996

Abstract

Rice Tungro disease (RTD) is a good pathosystem to study due to its large contribution to yield loss in Southeast Asian and the underlying synergistic interaction of two viruses. Comparing the outcome from our ODE-based deterministic and stochastic model formed using Gillespie's algorithm, the system's stochasticity resistance to was shown. Parameter scans used to test the effect of poorly characterised parameters on the disease dynamics showed their unequal importance to RTD dynamics and negative synergism. Lastly, different roguing intervals were tested for their cost-effectiveness in various situations, and the result showed a promising low-varied control over RTD.

Keywords: Plant epidemics, Rice Tungro disease, Stochastic modelling, Roguing, Disease control, Negative synergism

Introduction

It has been estimated that 16% of global rice yield loss is due to pathogens [1]. At a local scale, it can wipe out all of the rice cultivation, threatening food security and financial status of crop growers in many developing countries, such as in Southeast Asia. Apart from having economic and humanitarian importance, tracking crop epidemics can help reveal biological insights into interactions between plants-pathogens-vectors.

Rice can be invaded by more than one type of pathogen, and the co-infection can lead to a disease such as Rice Tungro Disease (RTD). RTD-causing annual yield loss can vary between 30-100% [2, 3], so it is one of the most devastating rice diseases [4]. It results from the co-infection of Rice Tungro Bacilliform Virus (RTBV) and Rice Tungro Spherical Virus (RTSV). Only when hosts have both viruses do they show strong symptoms, including stunted growth, reduced tiller numbers, and yellow to orange leaf discoloration [5]. The symptoms in the single RTBV-infected are milder, and there are no symptoms seen in the single RTSV-infected [5, 6].

The two viruses are mainly transferred by green leafhoppers (GLH; *Nephotettix virescens*) in semi-persistent manner. In the doubly infected, both of the viruses can be taken up together by GLH at 90-99% [5]. However, RTBV in the single RTBV-infected will not be taken up by GLH, while RTSV can be transmitted even when it is in the single RTSV-infected [6], so their relationship can be considered as helper-dependence (RTBV is a 'dependent virus', and RTSV is a 'helper') [3]. The differential symptom severity caused by the infection of either of them or both and the asymmetrical transmission conditions for both viruses make RTD a good system to study the effect of symptom severity and transmission dependency on the spread of each virus.

There have been a number of attempts to limit and prevent the RTD spreading. Some control measures include roguing (searching and removing infected hosts), using insecticides and developing of disease resistant varieties [7]. The aim of this study was to investigate the effectiveness of roguing as a RTD control measure. Roguing has a high accessibility, low related cost, and no risk of insecticide contamination and, therefore, is the simplest cultural control strategy usually performed by small-holder growers [8]. We set out to study the dynamics of RTD and the roguing control measure by creating a computational model (mathematical representation of a system) to test hypotheses and perform *in silico* experiments.

There were previous modelling studies of RTD using either stepwise (discontinuous) model by Holt & Chancellor (1996, [8]) and continuous model (ordinary differential equation (ODE)-based model) by Blas & David (2017, [9]). Holt & Chancellor only modelled the effect of roguing with a fixed interval and defined the roguing effectiveness based solely on the relative change in RTD incidence. However, roguing at increasing frequencies associates with the increased operation cost and the reduced yielding host number, and therefore, there is a trade-off between the cost of roguing and the yield. Thus, the economics of roguing should

be considered in addition to their disease-controlling ability, especially before it will be recommended to be implemented in the real world. This can be modelled as shown by Cunniffe et al (2014, [10]) stating that the optimal strategy depends on the relative value between the cost of roguing and the price of products. Blas & David compared two situations of roguing with the different probabilities of detection, but the probability was identical for hosts with every infection status (RTBV-singly, RTSV-singly, RTBV/RTSV-doubly infected). However, the obviousness of symptoms is different depending on the type(s) of viruses a host harbors [5], so the detection probability should vary accordingly [8].

Additionally, none of the models incorporated stochasticity, but the randomness often seen in natural events, either caused by the fluctuation in environment or population size, can change the dynamics of the disease [11, 12]. Especially when the overall disease dynamic comprises of many events related to many populations such as in RTD, the noise from each event may add up and deflect a trajectory away from deterministic behavior [13]. Environmental stochasticity can be ignored as the temperature and rainfall are relatively stable in most rice-growing countries in Southeast Asia. A recent work by Kim et al. (2019, [14]) formed a deterministic model that considered the effect of environment on the RTD dynamics (but simplified it by considering RTSV and RTBV as one virus population) and concluded that temperature must be more varied than what observed in their studied area to have an effect on the RTD incidence.

Therefore, in this study, we investigated how demographic stochasticity (a random change in population size due to the change-dependent nature of birth and death of individuals) changes the dynamics of disease by quantitatively comparing the host abundances produced the base deterministic model and the stochastic model developed using Gillespie's Direct method [15, 13]. Then, different key parameters in the stochastic model were scanned

over to qualitatively test their effect on RTD dynamics. Constructing the stochastic model of RTD and parameterizing relevant biological events can also reveal a how RTD pathosystem works, such as how the change in transmission rates due to co-infection affects the incidence of RTD and what conditions that lead to a potential competition between RTBV and RTSV. We then studied the cost-effectiveness of roguing strategies with different inter-rouge gaps when probabilities of detection were differentiated for each infectious status. Overall, this work then can partially reveal both the fundamental biological processes. and the practicality of stochastic modelling and roguing control.

Method

1. The model development and comparison

1.1. Base deterministic model with and without roguing

The ODE equations for Rice Tungro Disease (Equation (1) – (5)) were constructed based on the general model of plant virus synergism from Zhang et al. (2001, [16]). Individual rice hosts are divided into 4 compartments based on their infection status: non-infected or susceptible hosts (X), RTBV-singly infected hosts (Y), RTSV-singly infected hosts (Z), and RTBV/RTSV-doubly infected hosts (U) (Fig. 1; Table 1). In rice cultivation, it is common to transplant more than one individual rice plant together in a hole (a clump of rice plants, called a hill). However, we can assume one hill to be one plant as there is a very high within-hill spread due to their proximity [7]. As our focus was on the abundance host population to assess the effect of stochasticity and roguing, our model did not include the green leaf hopper (GHL) vector dynamics (the demographic changes, virus acquisition, and movement). We could also assume that the GLH population was in equilibrium with the virus populations, although this might not be perfect as the GLH transmit both viruses in semi-persistent way, allowing

overhanging inoculation source even after the original plant source from which GLH obtained the virus(es) has died. For simplicity, the latent period was also assumed to be equal to the incubation period as they are approximately of the same order (33 hrs-7 days and 7-14 days, respectively).

There are five types of demographic events, excluding roguing. For birth, the most common practices of rice planting involve making a regular pattern of holes (usually separated by 25x25 cm [17]) into which 3-5 rice seeds are dropped (drilling method) or 3-5 rice seedlings are transplanted (transplanting method) [18]. After certain time, rice growers may replant rice in holes that see no growth or further growth of rice seedlings by dividing rice from the nearby hill [8]. Thus, the birth rate of susceptible (X) is defined as $\boldsymbol{r(K-P)}$, where $\boldsymbol{r}$ is the rate at which re-(trans)planting of X occurs, $\boldsymbol{K}$ is the maximum rice host capacity in a certain area when the birth and death rate of X is zero (equivalent to the number of holes) and $\boldsymbol{P}$ is the current rice host abundance. The death of X, Y, Z, and U compartments occurs at rate $\boldsymbol{q, m, n, w,}$ respectively (Fig. 1; Table 1).

There are five types of viral transmission events. The transition X-Y and Z-U occurs when RTBV gets inoculated in X and Z, respectively. The vector may have acquired RTBV either from Y or U, and this leads to the different rate of successful transmission of RTBV to non-RTBV infected hosts (X and Z). If the source is Y, the rate is $\boldsymbol{p_1}$, but if the source is U, the rate is defined as $\boldsymbol{p_1 s_1}$, where coefficient $\boldsymbol{s_1}$ is the change in transmission rate of RTBV due to a source having RTSV. Without loss of generality, the rate of X-Z and Y-U transition can also be broken down into two components (with the rate $\boldsymbol{s_2}$ and $\boldsymbol{p_2 s_2}$). Lastly, the X-U transition occurs when a vector has fed on U and simultaneously inoculates both RTBV and RTSV into X, and this happens at rate $\boldsymbol{p_5}$ (Fig. 1; Table 1).

When included, roguing occurred with the conditions: 1) Take place within-field; each host represents each individual plant (hill), and 2) No replanting in place of rogued plants to reduce the risk of re-infection as the viruses can still survive in the remaining rice stubbles. A variable d_i was used to express the roguing effect in the model that take into account both compartment-specific probability of detection (e_i) and inter-rogue gap (g), in the form of equation (5) (Appendix 1)

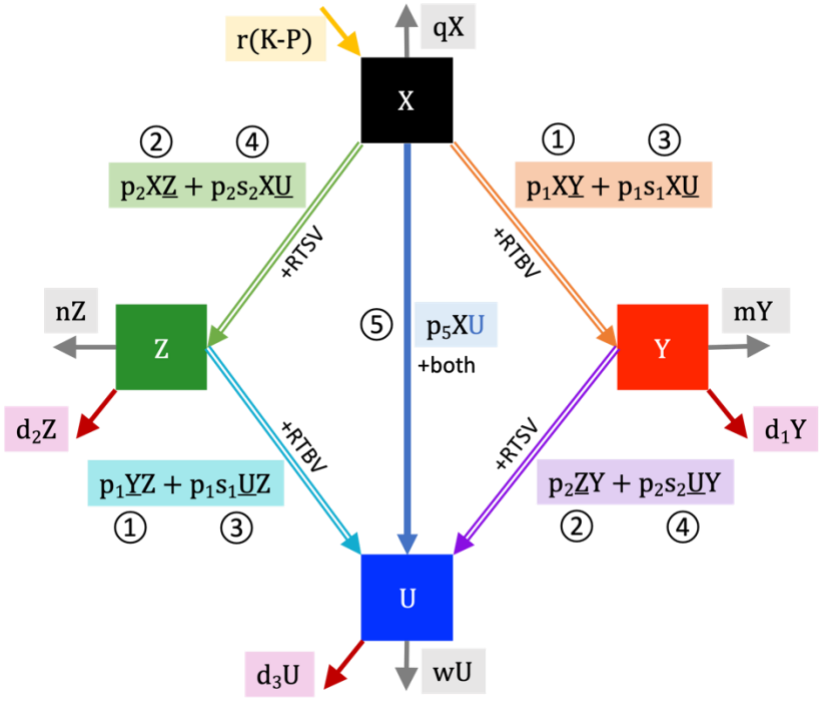

Figure 1: Model of Rice Tungro Disease (RTD) dynamics. Four host compartments are non-infected or susceptible hosts (X), RTBV-singly infected hosts (Y), RTSV-singly infected hosts (Z), and RTBV/RTSV-doubly infected hosts (U). The circled numbers correspond to the case of transmission shown Table 1. Five transmission events can occur, four of which have two components (=>) each with the different transmission rates depending on the source of virus(es). The transmission rate is p_1 for Y-acquired RTBV-containing vector, p_2 for Z-acquired RTSV-containing vector, p_1s_1 for U-acquired RTBV-containing vector, and p_2s_2 for U-acquired RTSV-containing vector. Only X-U transition can occur by the single type of event (->): vectors gain both viruses from U and transmit them onto X at rate p_5. All of the transmissions depend on the abundance of inoculum source (underlined) and of inoculated host. The birth rate of X depends on the planting rate (**r**) and the maximum host abundance when birth rate is zero (***K***), and it is negatively correlated with the current host abundance (P = X+Y+Z+U). Hosts in X, Y, Z, and U have natural death rate of q, m, n, and w, respectively. The three roguing-associated death rates are d_1, d_2, and d_3 for Y, Z, and U, respectively. They increase with the probability of detection (e_1, e_2, e_3) and decrease with inter-rogue gap (g) (equation (5)).

Equation (1) to (5)

$$\frac{dX}{dt} = r(K - P) - p_1(Y + s_1U)X - p_2(Z + s_2U)X - p_5UX - qX \quad (1)$$

$$\frac{dY}{dt} = p_1(Y + s_1U)X - p_2(Z + s_2U)Y - mY - d_1Y \quad (2)$$

$$\frac{dZ}{dt} = p_2(Z + s_2U)X - p_1(Y + s_1U)Z - nZ - d_2Z \quad (3)$$

$$\frac{dU}{dt} = p_2(Z + s_2U)Y + p_1(Y + s_1U)Z + p_5UX - wU - d_3U \quad (4)$$

$$d_i = \frac{1}{\left(\frac{1}{e_i} - \frac{1}{2}\right)g} \quad ; i \text{ is 1, 2, 3 for Y, Z, U, respectively} \quad (5)$$

Table 1: Explanation of events and parameters in the model

Compartments	**Abundance** (plants per area)			
X	Virus-free host (susceptible host)			
Y	RTBV singly infected host			
Z	RTSV singly infected host			
U	RTBV/RTSV doubly infected host (RTD-affected host)			
Virus transmission event	**Source**	**Transition**	**Parameter**	**Unit**
Case 1: +RTBV	Y	X to Y or Z to U	p_1	plant.day^{-1}
Case 2: +RTSV	Z	X to Z or Y to U	p_2	plant.day^{-1}
Case 3: +RTBV	U	X to Y or Z to U	(p_1s_1)	plant.day^{-1}
Case 4: +RTSV	U	X to Z or Y to U	(p_2s_2)	plant.day^{-1}
Case 5: +RTBV and RTSV	U	X to U	p_5	plant.day^{-1}
Change in transmission rate			**Parameter**	**Unit**
Change in transmission rate of RTBV due to a source previously being infected by RTSV			s_1	dimensionless
Change in transmission rate of RTSV due to a source previously being infected by RTBV			s_2	dimensionless
Other events or constants			**Parameter**	**Unit**
Host planting rate			r	day^{-1}
Maximum host abundance when birth rate is zero			K	Plants per area
Death rate of X			q	day^{-1}
Death rate of Y			m	day^{-1}
Death rate of Z			n	day^{-1}
Death rate of U			w	day^{-1}
Gap between roguing			g	day
Detection probability during roguing (for Y, Z, U, respectively)			e_1, e_2, e_3	dimensionless
Removal rate due to roguing (for Y, Z, U, respectively)			d_1, d_2, d_3	day^{-1}

1.2. The stochastic model with added roguing effect

For Gillespie's Direct Algorithm, the rates of all 13 possible events were added up to form the total rate. It was used as the rate parameter in the exponential distribution for estimating a time point that an event will happen, while the identity of the event that happened was randomly selected with the probability equal to its contribution to the total rate. Depending on which event occurred, the abundances of each compartment were updated accordingly (+1, -1, or 0) (Sup. Table 1). For each parameter set, 10 rounds of stochastic simulations were performed, and mean trajectories were found over a specified time over 500 days after planting to ensure that the steady state of the system was reached.

1.3. Model comparison

To test if demographic stochasticity was necessary for the RTD model, we compared the pair of host abundances produced by the deterministic and stochastic models input with the same set of parameters, randomly chosen from the ranges partially determined based on paper by Holt & Chancellor (HC1996) and Blas & David (BD2017) [8, 9]. (Sup. Table 3.2-3.3). Some parameters were only used in BD2017 paper, so they were fixed, while others were given a range that cover values from the two papers (Sup. Table 3.1). Some normalization for transmission rate parameters was needed to account for the difference in model development (Appendix 2). We used of ***K*** (the host capacity when birth rate is zero) = 10,000, which was the half of the value from BD2017, to reduce the time for simulation. Initial conditions were chosen from six combinations, representing different relative and absolute initial abundances. Since 135-day period is the average cropping period of rice (3 to 6 months), the ratios of host abundances at day 135 from the stochastic model (stoX135, stoY135, etc.) and from the deterministic model (detX135, detY135, etc) were calculated for each of the 100 comparative runs (the simulations using both models fed with the exact same parameter set). The ratios

falling outside 0.5 – 1.5 range were considered as the support for the need for stochasticity to be included.

2. Parameterisation

2.1. Investigation of the effect of unknown parameters

Parameter definite values or possible ranges were extracted from HC1996 and BD2017 paper. The parameters that were used in only one paper or agreed by both papers were automatically chosen as the default value (Sup. Table 2).

All of the other transmission-related parameters that were not agreed by the two papers; this included RTSV transmission rate from RTSV-singly infected plants (Z) ($\boldsymbol{p_2}$), RTBV/RTSV co-transmission rate from RTBV/RTSV-doubly infected plants (U) ($\boldsymbol{p_5}$), change in transmission rate of RTBV due to a source previously being infected by RTSV ($\boldsymbol{s_1}$), and change in transmission rate of RTSV due to a source previously being infected by RTBV ($\boldsymbol{s_2}$). Therefore, we either compared trajectories of two cases of the parameter (for $\boldsymbol{p_2}$ and $\boldsymbol{p_5}$) or formed two-way scanning (between $\boldsymbol{p_2}$ - $\boldsymbol{p_5}$ and $\boldsymbol{s_1}$ - $\boldsymbol{s_2}$) to study their effect on the RTD-affected host proportion at day 135 (proportion of U135) (Fig. 2).

2.2. Search for default set of an unrouged situation

We aimed to construct the conditions that produce high RTD incidence (high U proportion) from stochastic model to be used as the baseline for roguing effectiveness investigation. We then quantitatively chosen transmission-related parameter values to be the defaults for unrouged situation on the basis that: 1) They were in a range of relative values or absolute values quoted by the two previous literatures (Sup. Table 2) and 2) They gave a maximum or close-to maximum value of the proportion of U135.

Figure 2: Summary of parameterisation (Method 2). The parameter p_1 (RTBV transmission rate from the RTBV-singly infected) was fixed due to the consensus between the HC1996 and BD2017 paper. The Case I and II were formed based on the ratio p_2/p_1 from the papers to test the individual effect of p_2 (RTSV transmission rate from the RTSV-singly infected) on RTD dynamics, and the same was done for p_5 (Case III and IV). The two-way parameter scan was performed between p_2-p_5 to test the inter-dependency of their effect on RTD dynamics and ensure the conservativeness of the chosen values. Lastly, s_1 and s_2 (the change in transmission rate of RTBV or RTSV due to the host having the other virus, respectively) were scanned two-way for the same purpose. The suffix **d** represents the default status of a parameter, chosen to give a local peak value of U135 proportion (The proportion of RTD-affected hosts in current population at day 135) and were in the ranges cited by the two papers. In doing these, we can both investigate the effects of transmission-related parameters and search for the default set (p_{1d}, p_{2d}, p_{5d}, s_{1d}, s_{2d}) for further roguing investigation

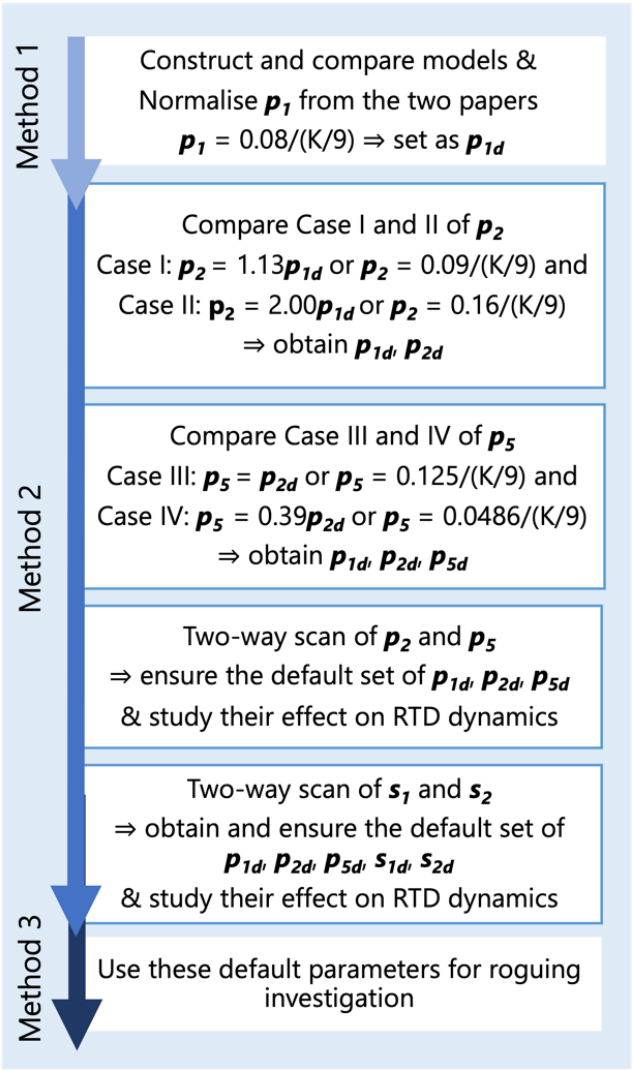

3. Effect of roguing gaps (g) and its error on the yield indices.

Following a search for an appropriate set of transmission-related parameters (p_{1d}, p_{2d}, p_{5d}, s_{1d}, s_{2d}), we tested the effect of roguing performed at different gaps (g; months), varied from half a month to 12 months, on each host compartment at average harvesting day (day 135). Yield losses due to RTD can arise by the death of rice plants, reduced tillers, and unfilled grains [19], and the RTBV-singly infected, RTSV-singly infected and RTBV/RTSV-doubly infected hosts (Y135, Z135 and U135, respectively) can still contribute to the yield, but to a lower extent compared individuals in healthy compartment (X135) on average.

The removal rate due to roguing (d_1, d_2, and d_3 for Y, Z, and U, respectively) was varied according to equation (5) (Appendix 1), using the probability of detection $e_1 = 0$ for Z (as there is no symptom development in Z), $e_2 = 0.7$ (mild symptoms), and $e_3 = 1.0$ (noticeable symptoms) [6]. To test the effectiveness of different roguing patterns, two indices were used.

3.1. Number of yielding host equivalent (*Yd*)

One way was to only consider the grain yield and assumed that there was no additional cost for roguing (neither for survey nor removal process). This is possible because 1) rice is relatively easy to remove and 2) based on the normal planting density of rice hill (20 x 25 cm^2 per hill), the rice population used in this simulation spanned over only a small area (Appendix 3.1), and so little human resource will be required.

For any roguing interval (g), we the defined Yd as the number of yielding host equivalent (equation (6)) as a function of the abundance at day 135 of healthy and infected hosts (X135, Y135, Z135 and U135, respectively). The potential yield loss varied greatly between rice varieties [19]; therefore, TN1 variety (Taichung Native 1), the most susceptible variety to RTD, was chosen for yield loss calculation. In fact, rice experiences a higher yield loss, if it gets infected by any of viruses earlier after planting, [5, 19] (Appendix 3.2). Therefore, each individual in Y135 did not contribute equally to the yield, and similar consideration applied to individuals in Z135 and U135. However, our current model could not provide the data on the age at which each host got infected. Thus, for each infected compartment, we averaged the percentage yield losses of TN1 rice cultivar infected at different time after planting (Appendix 3.2) and used it as yield coefficients (c_1, c_2, and c_3, for Y, Z, and U, respectively) in the equation (6). The most-yielding gap was g that produced the largest Yd.

$$Yd = X135 + c_1(Y135) + c_2(Z135) + c_3(U135)$$

$$= X135 + 0.46(Y135) + 0.78(Z135) + 0.12(U135) \quad (6)$$

3.2. Economics of roguing (***Econ***)

However, to extend the use of our model to a larger cultivation, it is useful to construct a framework that considers a cost of roguing and wasted agricultural inputs (representing the grain yield that can potentially be obtained from the rogued plants). Therefore, we formed another index ***Econ*** that considered the ratio between the cost of roguing per rice hill (***Cr***) and the price of grain yield per rice plant deducted by cost of input from one hill (i.e. net profit, ***Pr***), shown in equation (7). For each roguing gap (***g***), ***Cr*** increased with the number of roguing rounds happened before day 135 (***N***), which can be defined as ***N*** = (135/***g***). ***N*** was allowed to be non-integer to capture the continuous nature of our model. The most-cost effective gap was ***g*** that produced the greatest ***Econ***.

$$Econ = Yd - N\left(\frac{Cr}{Pr}\right) = Yd - \frac{135}{g}\left(\frac{Cr}{Pr}\right) \quad (7)$$

3.3. Effect of yield coefficient error on the optimal roguing pattern

All the yield coefficients (***c*₁**, ***c*₂**, and ***c*₃**, for Y, Z, and U, respectively) were obtained by averaging the highly varied values of yield losses (of TN1 infected at different ages), but some or all of them could become critical variable(s) in determining the best strategy for roguing control on TN1 rice population (based on ***Econ*** index). Thus, we tested how different levels of percentage error of the yield coefficient of the host compartment that contributes most to the yield affect ***Econ***, by allowing each of them to vary within 5%, 10%, and 25% limit. The distribution of ***Econ*** calculated using 1000 randomly selected values of the coefficients were plotted for each combination of %error and ***Cr/Pr***.

Result

1. Stochastic and deterministic model comparison

All of the ratios between host abundances at day 135 from the stochastic model and from the deterministic model (e.g. stoX135/detX135, stoY135/detY135, etc.) produced from 100 comparative runs were mostly between 0.5 to 1.5 (Fig. 3A-B). Together, only 38 out of 400 ratios were out of this range, and they were from 22 independent comparative runs, all of which using initial condition as X0=1000, Y0=1=Z0, and U0=0. The other initial condition sets (Sup. Table 3.3) with greater-than-1 Y0 and Z0 led to the production of virtually similar proportions of all host compartments at day 135 from the two models. There was only one run that produced all ratios of host abundances that were out of this range; we called the parameters used in this run the "extreme set" (Sup. Table 3.4).

We hypothesized that the extinction of at least one host compartment in at least one stochastic run using this set of parameters led to the great deviation from the outcome from the deterministic model. We then observed progress curves of all hosts from 10 independent stochastic simulations using this "extreme" set of parameters and compared it with the curve from the deterministic model. The result (Fig. 4A) showed that, in deterministic run, although the RTSV-singly infected (Y) were greater than the RTSV-singly infected (Z) at the steady state, Z did not go extinct. In contrast, in 2 out of 10 stochastic runs, Z faced the extinction and RTD-affected plants (U) were virtually not produced, which together led to the slower drop of the susceptible (X) (Fig. 4B). However, Y was higher in these 2 runs, eventually causing X to stay at the steady-state value (~0.2), similar to the other simulations. The diverging Y trajectories (0.8 vs 0.2 of the steady-state population) also showed the Z-dependent Y abundance, potentially reflecting the negative effect from RTSV on the survival of RTBV in the population, and vice versa.

A)

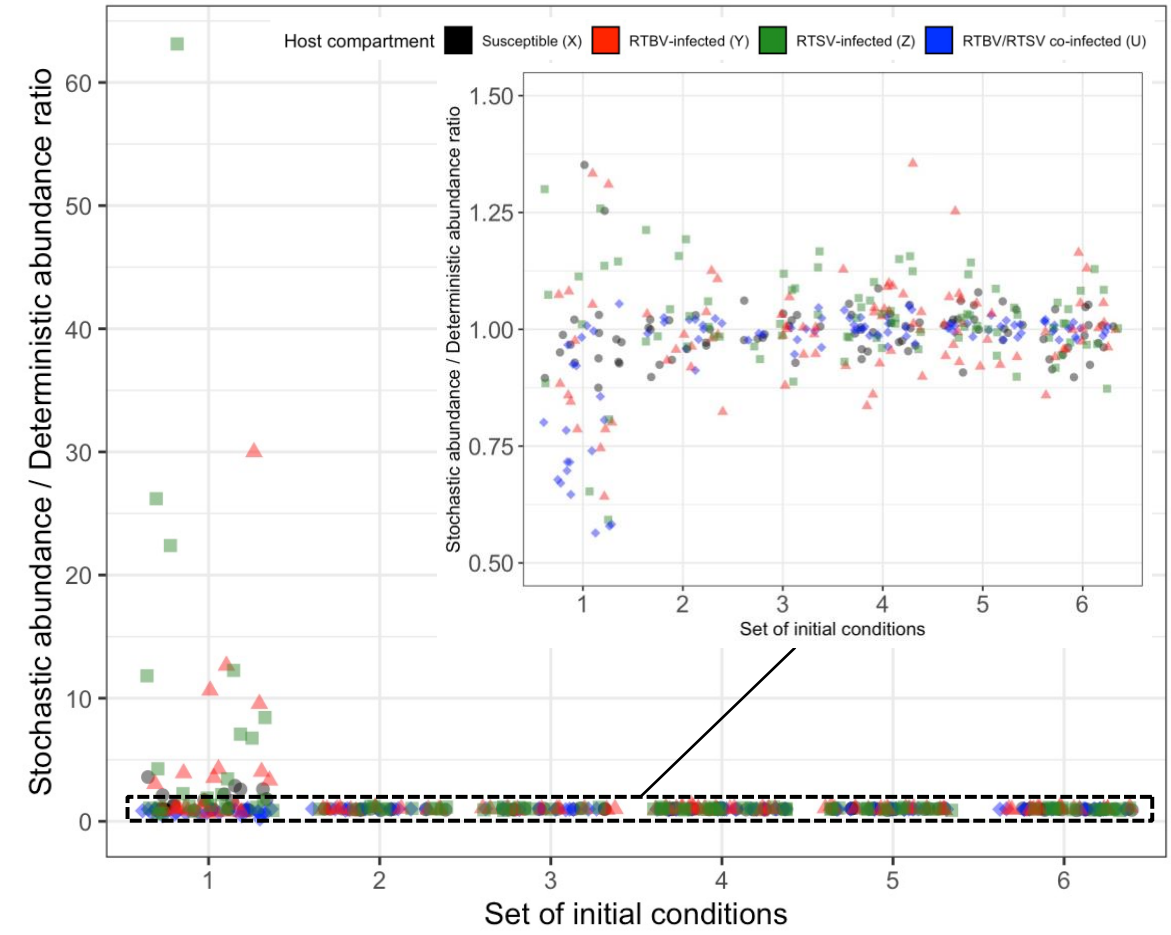

B)

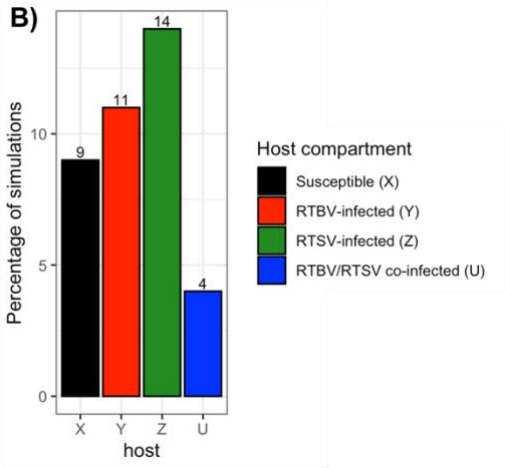

Figure 3: The comparison between deterministic and stochastic model. A) The distribution of ratios between stochastic and deterministic host abundance for all 4 host compartments. The same sets of random parameters were used in simulating the RTD dynamics from both model (n=100). X-axis represents six sets of initial conditions randomly chosen for each comparative simulation (Sup. Table 3.3). A large plot shows the ratio for all 100 simulations for each host compartment, separated by color as in the legend, while the inset shows only ratios that stayed within 0.5 – 1.5 range, which accounted for ~90% of all ratios. The RTSV-infected (Z) varied the most, hitting >60 at one of the simulations, followed by the RTBV-infected (Y). Only initial condition set 1 (X0=1000, Y0=1=Z0, U0=0) created out-of-range ratios, reflecting the limited role of demographic stochasticity in Rice Tungro Disease pathosystem. **B) Percentage of simulations that produced ratio between stochastic and deterministic host abundance that were outside 0.5-1.5 range.** RTBV/RTSV co-infected (U) was the most resistant to stochasticity as only 4% of all simulations give ratio out of the range. The most deviated ratios belonged to Z compartment, followed by Y.

Using other initial conditions with this "extreme" set (Appendix 6) showed that only if either Y or Z started off with as small population as 1, the stochasticity can play a role in shaping the disease progression. U0 was proved to be irrelevant to the degree of stochasticity subjectivity as the comparative runs with initial condition with U0=0 (set 2-3; Sup. Table 3.3) did not produce any out-of-range ratios, similar to other sets that had non-zero U0. In general, we then can conclude that RTD pathosystem was insensitive to demographic stochasticity.

Figure 4: RTD progress curve produced using the "extreme" parameter set that produced all-host out-of-range ratios (more than 1.5 or less than 0.5).

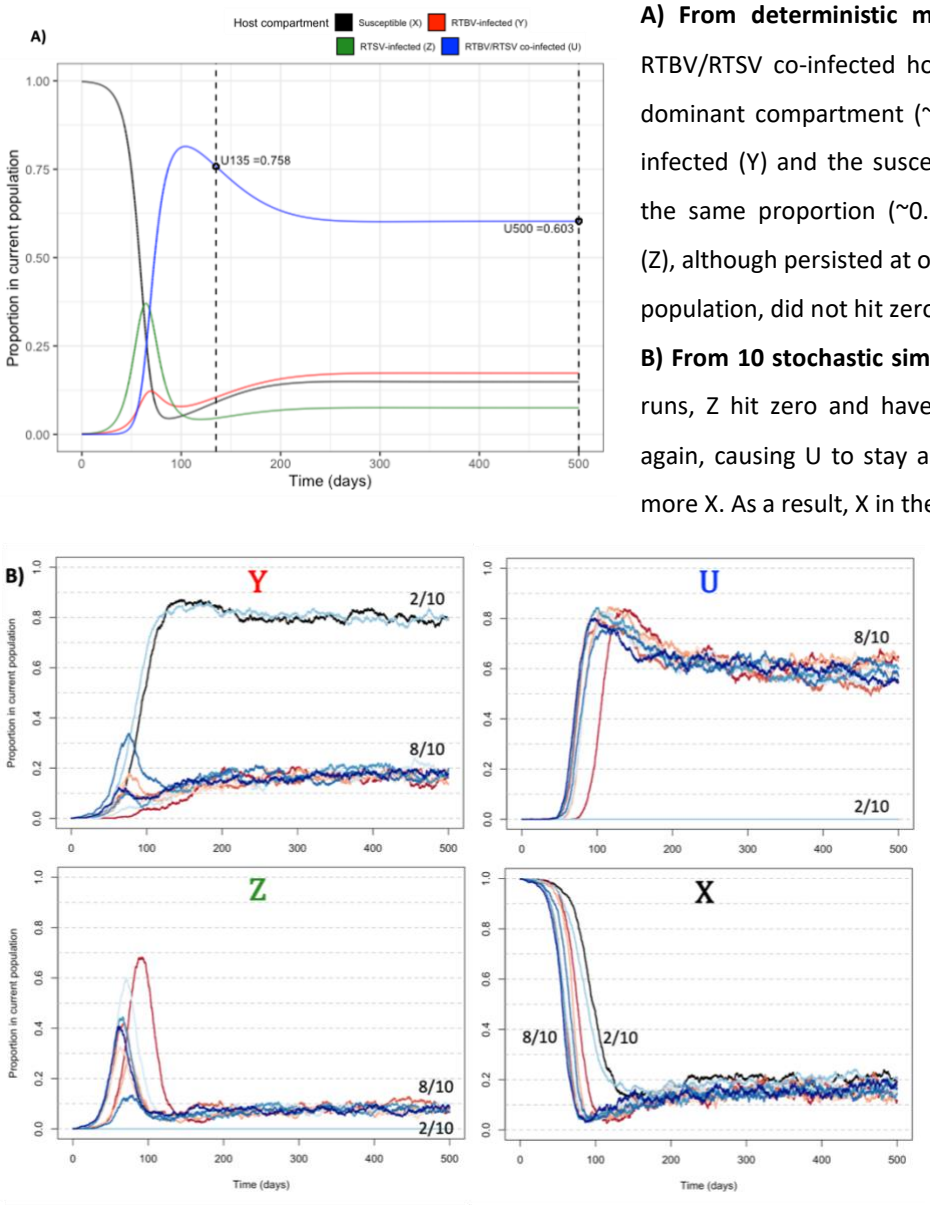

A) From deterministic model. At steady state, RTBV/RTSV co-infected hosts (U) were the most dominant compartment (~0.60), while the RTBV-infected (Y) and the susceptible (X) were around the same proportion (~0.15). The RTSV-infected (Z), although persisted at only ~0.07 of the current population, did not hit zero.

B) From 10 stochastic simulations. In 2 out of 10 runs, Z hit zero and have never been produced again, causing U to stay at zero and Y to occupy more X. As a result, X in these 2 runs dropped later but hit the similar proportion at steady state to the other 8 runs. This parameter set (Sup. Table 3.4), supported the need for the demographic stochasticity in RTD model and showed the pressure from one virus on the survival of the other.

For the purpose of this study, we used the stochastic model with the initial condition Y0=Z0=10 (0.1% of $\boldsymbol{K}$) and U0=1 (0.01% of $\boldsymbol{K}$) for further investigation. This set would not cause the diverging cases (i.e. no extinction of any of the host populations); however, this represented the more likely scenario of the Rice Tungro Disease spread problematic to agriculture.

2. The effect of RTSV single transmission rate (p_2) and RTBV/RTSV co-transmission rate (p_5) on the proportion of RTD-affected hosts (U)

2.1. Individual effects on RTD

In two cases of varied $\boldsymbol{p_2}$ (case I: $\boldsymbol{p_2}$=1.13$\boldsymbol{p_{1d}}$=0.09/($\boldsymbol{K}$/9) and case II: $\boldsymbol{p_2}$=2.00$\boldsymbol{p_{1d}}$= 0.16/($\boldsymbol{K}$/9)), the trajectories of U compartments were similar (Fig. 5A), and U were also the most dominant compartments at day 135 and day 500 in both cases (Sup. Fig. 1). Practically, the number of RTD-affected hosts during the harvesting period (U135) was 352 and 360 plants per area for case I and case II, respectively. Therefore, the two cases allowed similar spread of RTD. Thus, we used $\boldsymbol{p_{2d}}$ equal to the mean of the two cases (0.125/($\boldsymbol{K}$/9)) for further investigation of $\boldsymbol{p_5}$.

With default $\boldsymbol{p_{1d}}$ and $\boldsymbol{p_{2d}}$, $\boldsymbol{p_5}$ from the two cases (case III: $\boldsymbol{p_5}$=$\boldsymbol{p_{2d}}$=0.125/($\boldsymbol{K}$/9) and case IV: $\boldsymbol{p_5}$=0.39$\boldsymbol{p_{2d}}$=0.0486/($\boldsymbol{K}$/9)) had a slightly wider effect than $\boldsymbol{p_2}$, but still produced similar trajectories of U proportion (Fig. 5B) and had U as the most dominant compartment (Sup. Fig. 2). The actual number of U at day 135 (U135) was 352 and 360 plants per area for case III and case IV, respectively. Therefore, the two cases of $\boldsymbol{p_5}$ also allowed similar spread of RTD. We then considered the mean of the two cases (0.086/($\boldsymbol{K}$/9)) as the default parameters for $\boldsymbol{p_5}$.

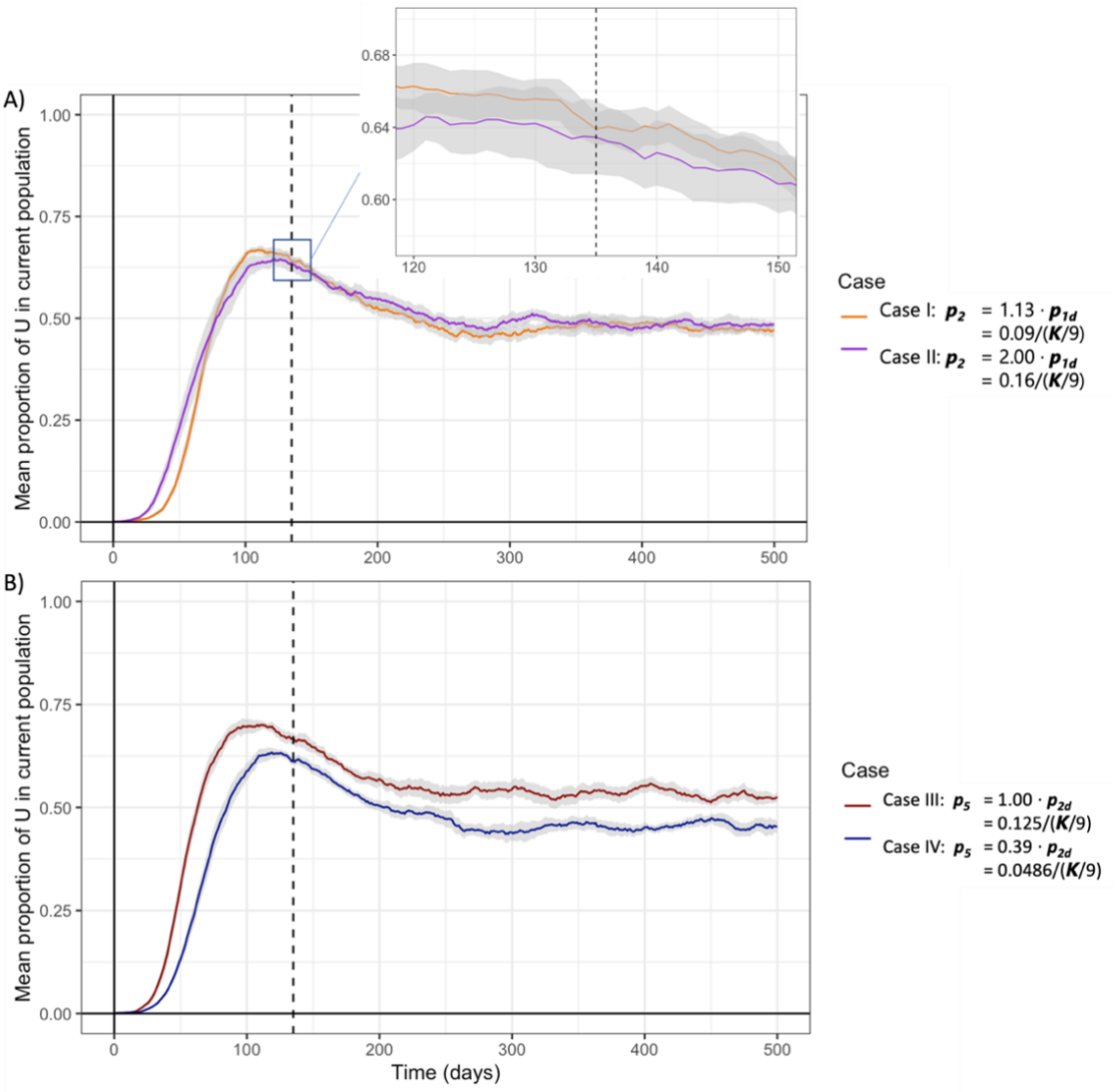

Figure 5: Comparison of the mean trajectories of RTBV/RTBV doubly infected host (U) proportion in current population (X+Y+Z+U) over 500 days. Grey areas represent SD (n =10). Dashed line was at day 135. **A) Two cases of p_2.** All parameters were identical between two cases, except p_2. The inset shows the closed-up of U135 proportion for both cases. The highly similar trajectories can be seen. Therefore, the mean of p_2 from both cases (0.125/(*K*/9)) was used as p_{2d} in combination with p_{1d} = 0.08/(*K*/9) for the subsequent parameterisation of p_5. **B) Two cases of p_5.** All parameters were identical between two cases, except p_5. The similar trajectories can be seen. Therefore, the mean of p_5 from both cases (0.086/(*K*/9)) was used as p_{5d} in combination with p_{1d}=0.08/(*K*/9) and p_{2d}=0.125/(*K*/9) for parameterisation of s_1 and s_2.

2.2. Combined effect and the strength of individual effects

According to the p_2-p_5 two-way scan outcome (Fig. 6), U135 proportion only varied within from 0.60 to 0.70, so the combined effect of these transmission parameters on U135 proportion was also non-significant.

The p_2-p_5 two-way scan outcome (Fig. 6) also showed that U135 proportion was less influenced by p_2 compared to p_5 i.e. the horizontal gradient was steeper than vertical one. This may be because increased p_5 (RTBV/RTSV co-transmission rate) directly allows more the transition into U from X (Fig. 1), whereas an increased p_2 (RTSV single transmission rate) can suppress Y production as X is converted to Z more often than Y (Fig. 4B). Consequently, the smaller source of RTBV partially offsets the beneficial effect of increased p_2 on the rate of U production.

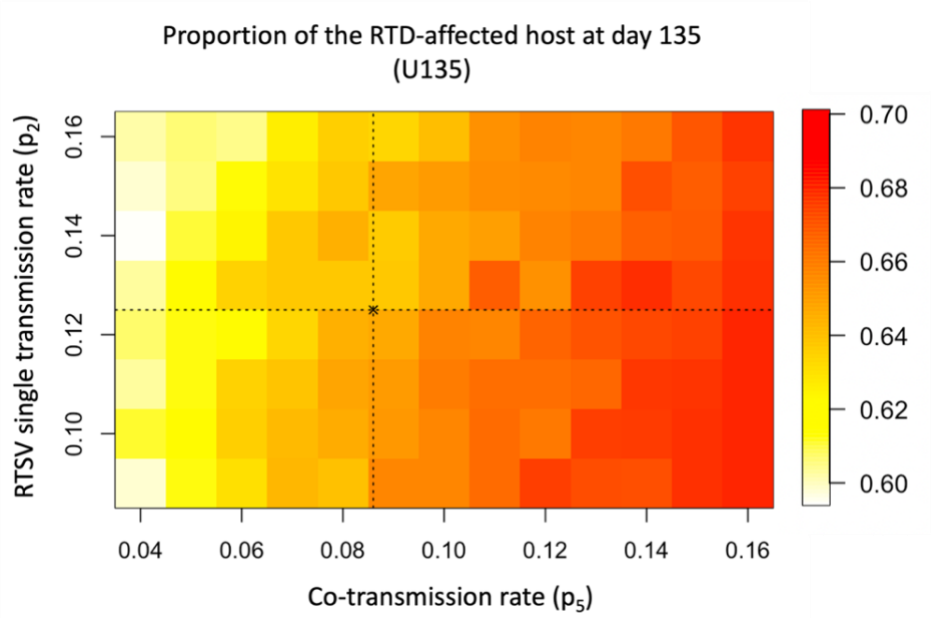

Figure 6: The two-way scan outcome of RTSV single transmission rate (p_2) and co-transmission rate (p_5). The ranges of scanning covered the cited values from HC1996 and Bd2017 paper. Color scales represents the value of the proportion of RTD-affected host at day 135 (U135) as shown in the legend. The range of U135 was relatively narrow (0.60-0.70), so their joint effect on RTD were not significant. The horizontal color gradients were steeper than vertical ones, reflecting the greater influence of p_5 compared to p_2 on U135 proportion due to the contrasting effect of increased p_2 on U production. Dashed lines marked p_{2d} and p_{5d} equal to 0.125/(K/9) and 0.086/(K/9), respectively. The black cross (×) represents U135 proportion, given by this pair, which was 0.64. Although it was less than the mean of the U135 outcome from this plot (0.65), optimising this pair would not significantly increase RTD incidence. Therefore, the previously obtained p_{2d} and p_{5d} can be used for the investigation of s_1 and s_2.

3. The effect of the change in transmission rate of RTBV or RTSV due to the host having the other virus (s_1 and s_2, respectively) on the proportion of U135

3.1. Combined effect and the strength of individual effects

The U135 proportion from $\boldsymbol{s_1}$-$\boldsymbol{s_2}$ two-way scan using the previously-obtained pair of $\boldsymbol{p_{2d}}$ and $\boldsymbol{p_{5d}}$ (0.125/(K/9) and 0.086/(K/9), respectively) showed that change in transmission rate of RTBV due to the host having RTSV ($\boldsymbol{s_1}$) had a greater impact on the outcome i.e. the vertical gradient was steeper than the horizontal one (Fig. 7). This was likely because the values of the transmission rate of RTBV ($\boldsymbol{p_{2d}}$) used in the scan was more than the transmission rate of RTSV ($\boldsymbol{p_{1d}}$), so Y was fewer than Z (Appendix 4). Consequently, the production of U was more limited by the abundance of Y than it was by the abundance of Z. Increasing the overall transmission rate of RTBV (by increasing $\boldsymbol{s_1}$), therefore, allowed a greater change in U compared to increasing overall transmission rate of RTSV (by changing $\boldsymbol{s_2}$ with the same scale).

In addition, the outcome showed a strong negative relationship between the two viruses. The support was that, focusing on that very low $\boldsymbol{s_2}$ values (Fig. 7), increasing $\boldsymbol{s_1}$ increased the proportion of U135 at first, then the trend reversed (Sup. Fig. 3). This probably mean that, for any $\boldsymbol{s_2}$ values, the initial increase in $\boldsymbol{s_1}$ from very low values allowed RTD to persist better because a sufficiently high abundance of RTBV was in the system. However, a system with too high $\boldsymbol{s_1}$ means that RTBV transmission can be enhanced in U too excessively that the negative effect from RTBV on the survival of RTSV resulted in reduced RTSV, leading to the overall reduced U. This hypothesis was supported by Y135 and Z135 two-way scan outcome (Sup. Fig. 4) that show that they were dominant at different regions of the plots.

3.2. Individual effects on RTD

The two-way s_1-s_2 scan outcome showed that U135 was pushed to be close to 0.38 (×-marked U135 in Fig. 7), when s_1 and s_2 was equal to the means from the two papers (HC1996 and BD2017) of 0.458 and 0.500, respectively. This was much lower than the U135 proportion mean from this scan (0.47). Thus, this (s_1, s_2) pair was not good default parameters to be paired up with the default p_{1d}, p_{2d}, and p_{5d} for further roguing investigation, especially when considering the fact than U500 was always lower than U135 (Fig. 4-5 and Sup. Fig. 1-2).

To re-evaluate them, we varied one of the parameters at a time, so that we adhered to the cited ranges as much as possible. The one-way scanning of s_1 or s_2 with the other one being fixed at their previous default value showed that when s_1 =0.458, varying s_2 had a little effect on the outcome (Fig. 8A), varying s_1 allowed the proportion of U135 to change dramatically from less than 0.2 to more than 0.6, while fixing s_2 at 0.500 (Fig. 8B), further supporting the greater influence of s_1. Therefore, we changed s_{1d} to 0.75, as it did not exceed the value of s_1 equivalent cited in the two papers and was able to push U135 to almost its maximum value from the s_1 scanned range (Fig. 8B).

4. Effect of roguing gaps (g) and its error on the yield indices.

Overall, after all parameterisation steps, we have obtained the default set of transmission parameters suitable for investigation of roguing effectiveness (Appendix 5). The progress curve from deterministic and stochastic model both showed that more than half of the current host population were co-infected by RTBV and RTSV (having RTD) (Fig. 9, Sup. Table 4)

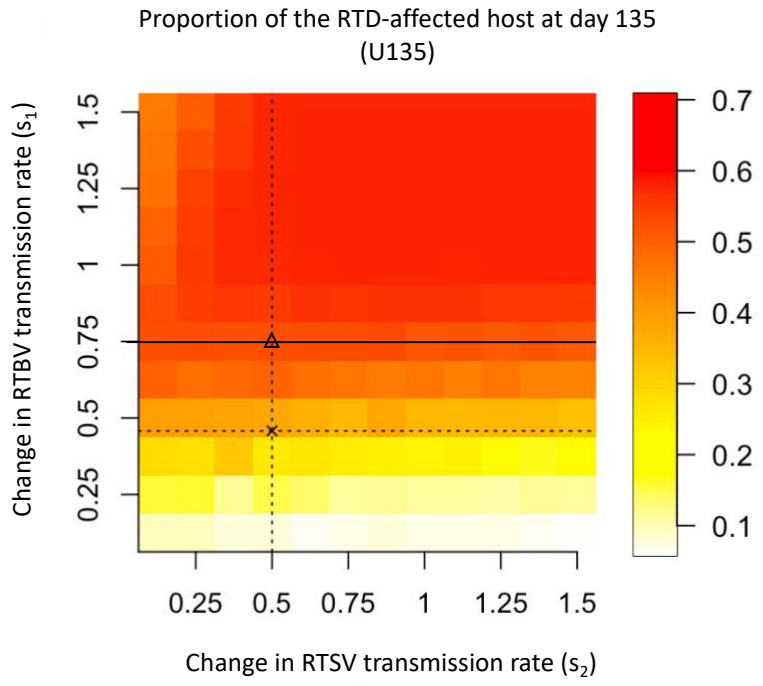

Figure 7: The two-way scan outcome of the change in RTBV transmission rate (s_1) and in RTSV transmission rate (s_2) due to an inoculum source having the other virus (i.e. the source is U) compared to having one type of virus. Color scales represents the value of the proportion of RTD-affected host at day 135 (U135) as shown in the legend.

Result 3.1: Due to a steeper vertical gradient, s_1 had weaker influence on U135 compared to s_2. A strong negative-relationship zone was seen when the value of s_2 was low and s_1 was high. **Result 3.2:** Black dashed lines are marked at s_1 and s_2 equal to 0.458 and 0.500, respectively. A cross (×) represents U135 proportion, given by this pair, which is 0.38 and this was considered as non-optimised as it was less than the mean of 0.47. Therefore, a new s_1 was selected to be 0.75 (solid line) based on the one-way scan of s_1 and s_2 and cited ranges in HC1996 and BD2017. Thus, (s_{1d},s_{2d}) equals to (0.75,0.50), giving out a reasonably high U135 marked by an open triangle (△), was then used with the previously-obtained (p_{1d}, p_{2d}, p_{5d}), for further roguing investigation.

4.1. Effect of roguing gaps (g) on the proportion of host compartments

The one-way scan outcome of the inter-rogue gap (***g***) 0.5 to 12 months showed that the more frequent roguing (decreasing ***g***) caused a decrease in the proportion of RTD-affected hosts at day 135 (U135) and a mild decrease in that of RTBV-infected hosts (Y135), but a noticeable increase in the proportion of RTSV-infected hosts at day 135 (Z135) (Fig. 10). This was expected as Z did not get rogued, while U and Y were rogued with 1.0 and 0.7 probability of detection, respectively. As the gaps got shorter, apart from the increasingly lower accumulative death rate of Z, the lower Y that represented no or smaller source of RTBV also slowed down the conversion of Z to U (slower Z-U transition; Fig. 1), leading to more

accumulation of Z over 135 days. The X-Z transition may also be accelerated, supported by the fact that X135 proportion was overall barely changed, while the X-U and X-Y transition must have been slower to lower U and Y in the population.

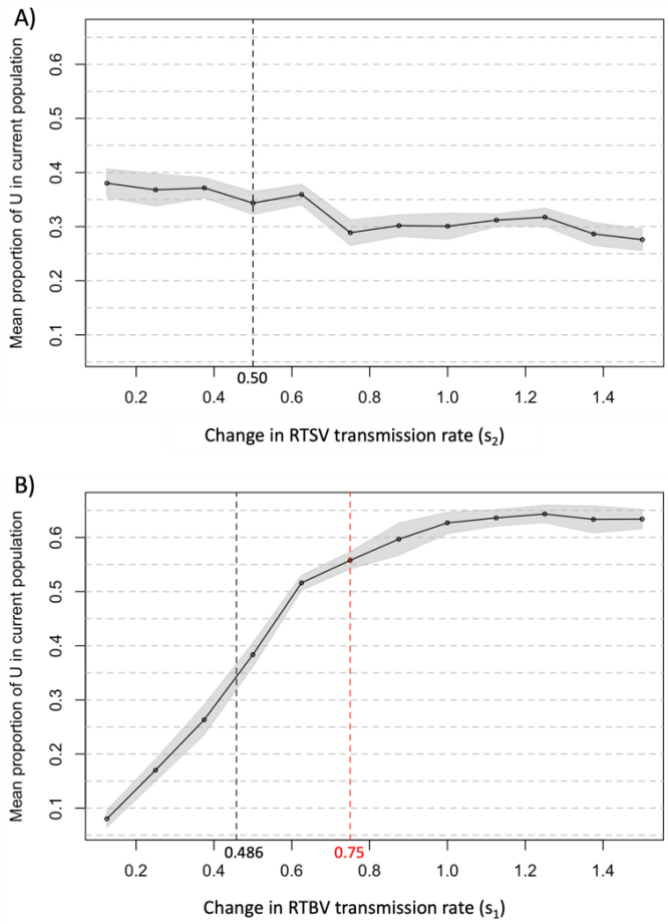

Figure 8: The plot of the mean proportion of U135 at different s_1 and s_2. Grey shaded areas represent SD (n = 10) **A) Scan of s_2 with s_1 fixed at 0.458.** A black dashed line represents the mean value of s_1 from the two papers (0.50). Varying s_2 has little effect on the proportion of U135 (stayed between 0.25-0.40). Therefore, s_2 = 0.50 was kept as the default. **B) Scan of s_1 with s_2 fixed at 0.500**. A black dashed line represents the mean value of s_2 from the two papers (0.458). The proportion of U135 increased greatly from 0.05 to 0.65 when s_1 moved from 0.125 to 1.50. Therefore, 0.75 (a red dashed line) was chosen as a new default s_1 as it was the maximum s_1 quoted from the two papers and can push U135 proportion to 0.55.

4.2. Effect of roguing gaps (g) on the yield indices

In the case that we assumed no related cost due to roguing, the potential number of yielding host equivalent (***Yd***) suggested that the best strategy was the smallest inter-roguing gap, as expected (Fig. 11A, Sup. Fig. 5.1). It increased the yield by almost 3.0-fold, compared to ***Yd*** of unrouged situation (276 plants per area). There was a little benefit (increased less than 35% of unrouged ***Yd***) from roguing every 6 to 12 months.

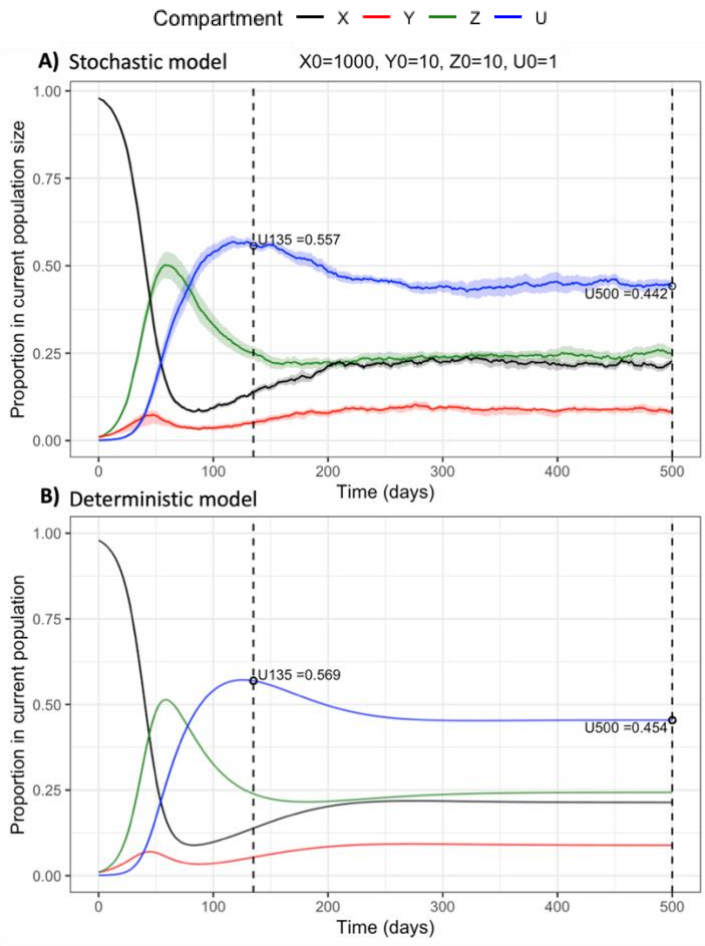

Figure 9: The progress curves of RTD dynamics over 500 days, showing the susceptible (X), the RTBV-infected (Y), the RTSV-infected (Z) and the co-infected (U), color-coded as in the legend. Dashed lines marks day 135 and day 500. The default parameters were selected following Method 2 (values shown in Appendix 4). **A) From stochastic model. B) From deterministic model.** This initial condition set (X0=1000, Y0=10=Z0, and U0=1) reduced the effect of demographic stochasticity, so the shape of all curves from the two models was the same, although the exact values of U135 and U500 were slightly lower in stochastic model. Overall, this was a good unrouged situation as U135 was reasonably high and all parameters stayed in previously cited ranges from HC1996 and BD2017 paper.

However, in most cases, the different conclusion was reached when we looked at Economics of roguing (***Econ***), which considered the cost of roguing relative to the price per yield from an individual host (***Cr***/***Pr***) (Fig. 11B). When ***Cr*** was more than 10-fold to 60-fold of ***Pr***, the best roguing strategy was changed from 0.5- to 1.0-month gap. If ***Cr***/***Pr*** was 70 or 80, it was pushed further to 1.5-mth gap due to the penalisation from the expensive accumulative cost of the higher number of rouging when the gaps were small. Although the trade-offs can be clearly seen (e.g. when ***Cr***/***Pr*** = 80, roguing every 1 or 2.5 mths gave the same index ***Econ***), the values of ***Econ*** were relatively close to each other (within 50 units) when the gaps were between 1.0-2.5 mths for ***Cr***/***Pr*** = 60 to 80. Thus, deciding the best gap at these ratios of trade-off can be affected by the uncertainty in yield coefficients, especially for the compartment Z, the most contribution to the index ***Yd*** (Sup. Fig. 5.2).

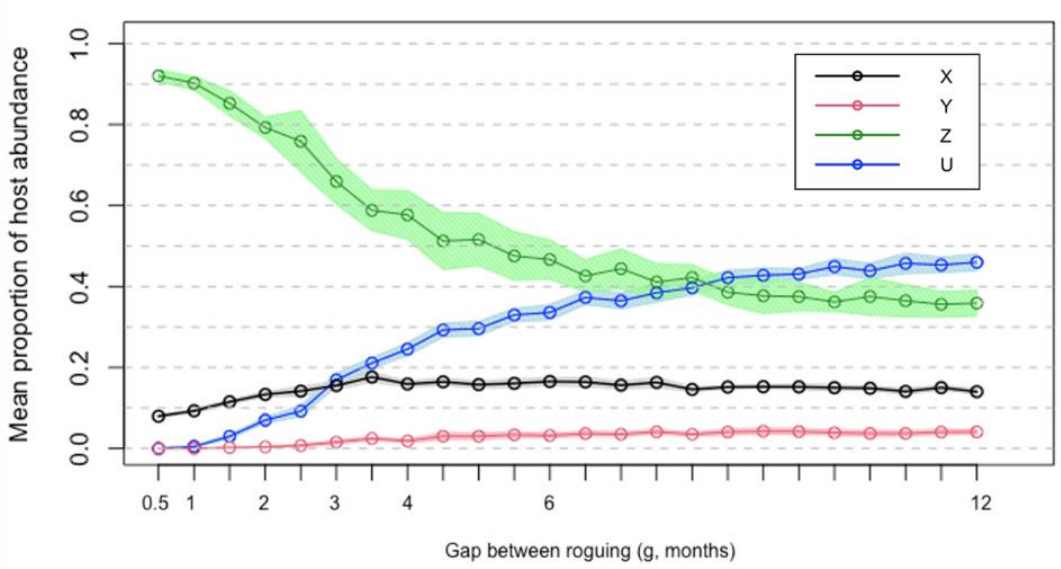

Figure 10: Mean proportion of all four compartments for different inter-rogue gaps (*g*). The proportion of the susceptible (X), the RTBV-infected (Y), the RTSV-infected (Z) and the co-infected (U) at day 135 were shown in black, red, green, and blue lines, respectively, with SD (n = 10). The gap between each roguing operation was increased by half-a-month step from 0.5 to 12 months. As the gap widened, Z135 changed most dramatically, decreasing from around 90% to 30%, while Y135 and U135 increased from non-existent to around 5% and 45%, respectively. X135 increased from 10% to 20% when the gap went from half a month to 3.5 months due to the reduction in Z135. A subsequent mild decreasing trend of X135 after that point was contributed by increasing U135 and Y135.

4.3. Effect of yield coefficient error on the best roguing gaps

Using random values of the Z135 yield coefficient (c_2), within either ± 5%, 15%, or 25% error range from the default 0.78, the spreads of the most cost-effective gaps (g_{best}) from 1000 cases for each combination of %error and ***Cr***/***Pr*** were wider with increasing %error as expected (Fig. 12). It was also wider with increasing ***Cr***/***Pr*** ratio as ***Econ*** at various ***g*** were closer when the ratio increases (Fig. 10B). The widest spread was seen with 25% error when ***Cr***/***Pr*** = 80; 685 out of 1000 cases did not give the same g_{best} seen in the corresponding no-error situation.

Despite changes in individual cases, most collective conclusions of g_{best} at each ***Cr***/***Pr*** ratio were not changed (0.5, 1.0, and 1.5 mth for ***Cr***/***Pr*** = 0, 10-60, and 70-80, respectively). The exception was only when ***Cr***/***Pr*** = 70; slightly more cases of c_2 with 15% (334 vs 299) and 25% error (325 vs 294) shifted g_{best} from 1.5 to 1.0 mth. This was slightly surprising as the

shifting did not happen with ***Cr***/***Pr*** = 80 even if the values of ***Econ*** at ***g*** = 1.5 and 2.0 mth were closer to each other than the shifting pairs.

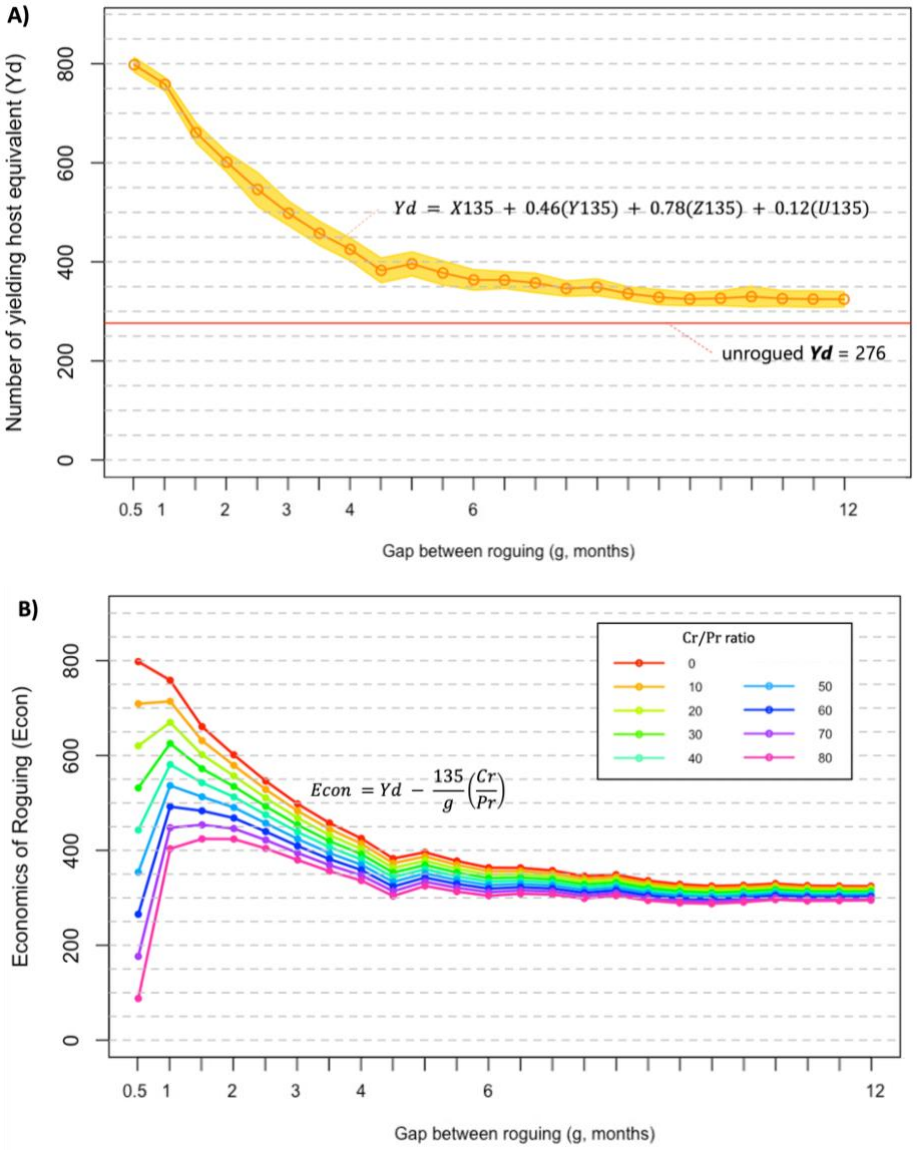

Figure 11: Assessing Effectiveness of roguing based on different yield indices. A) Number of yielding host equivalent (*Yd*) represents the sum of the number of each host compartment multiplied by their average yield contribution. Yellow area represents SD (n=10). 15-day (half a month) gap was the most effective, increasing the yield by almost 3 times of unrouged ***Yd*** (This red horizontal line)**.** Benefit from roguing every 6-12 months were limited to no more than 35% increase. **B) Economics of roguing (*Econ*)** considered the ratio between the cost of roguing and price of rice (***Cr***/***Pr***), which was set between 10 to 80. Red line represents when the ratio was 0, which was equivalent to ***Yd*** (Fig. 11A). 1-month gap was the most cost-effective (g_{best}) when ***Cr***/***Pr*** was between 10-60, while it was 1.5-month gap if ***Cr*** was 70-80 folds of ***Pr***.

Overall, ***Econ*** is relatively insensitive to the error c_2, and this property can be expanded to the error in individual yield coefficients of X135, Y135, and U135 as well as they contributed much less to ***Yd*** (and ***Econ***) (Sup. Fig. 4), but the combined effect of the errors may not be insignificant.

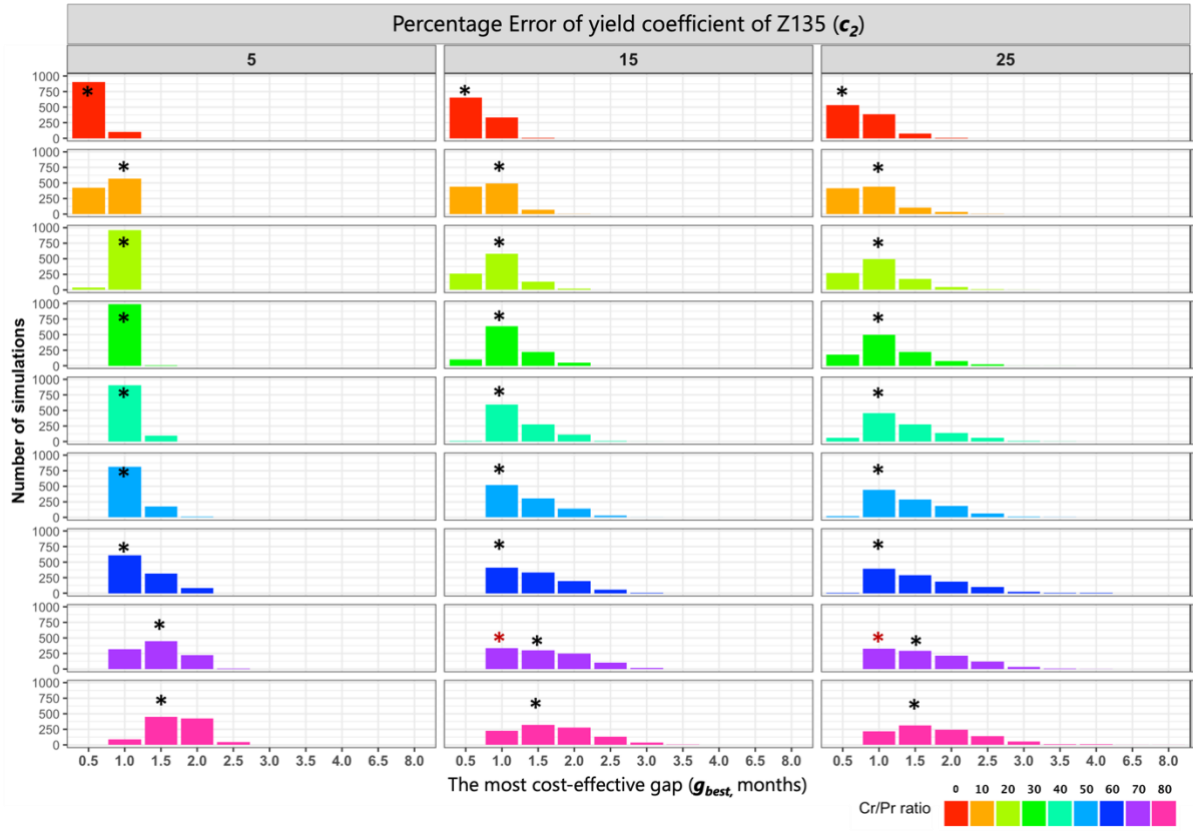

Figure 12: The distributions of the most cost-effective inter-rogue gaps (g_{best}, months) decided based on the index *Econ* calculated with the randomly selected value of Z135 yield coefficient (c_2) associated with different %error (5%,15%, and 25%). The distributions were separately shown for each ***Cr***/***Pr*** ratio (0-80), color-coded as in the legend. The black asterisks (*) shows g_{best} when c_2=0.78 (no error) for each ratio. A more diverse case of g_{best} (wider spread) was seen in cases with a higher %error and a higher ***Cr***/***Pr.*** At the most extreme (25% error and ***Cr***/***Pr*** =80), only 315 out of 1000 cases still suggested 1.5 mth as g_{best} (although it was still the most prominent g_{best}), and as high as 4.0 to 8.0-mth gap were suggested as g_{best} in 14 cases. However, collectively based on 1000 cases of c_2 for each combination of ***Cr***/***Pr*** and %error, most conclusions were not changed; at 5% error, no change in the optimal gap was seen, but 15% and 25% error caused the slight shift at ***Cr***/***Pr*** = 70 from 1.5 to 1.0-month gap (red asterisks *). Overall, ***Econ*** was an error-resistant index for assessing the cost-effectiveness of inter-rogue gaps.

Discussion

1. RTD dynamics is resistant to demographic stochasticity

Generally, random extinction can change the steadystate proportions of host compartments [20, 21], but our comparison between deterministic and stochastic model showed that it is hardly possible in RTD pathosystem (Fig. 3). This may result from the fact that the production of the RTBV-infected (Y) or the RTSV-infected (Z) was contributed by two components, one of which was independent of its size, and that the production of the co-infected (U) was contributed by three pathways, two of which did not depend on its size (Fig. 1). This means that, as long as only one of them went extinct, there are always influxes into all the infected compartments (Sup. Fig. 6). The extinction of two infected compartments can change the RTD dynamics more noticeably, but it is even more unlikely to happen.

2. The importance of each transmission parameter is different

The study of effects of the transmission rates and the change in that due to the co-infection showed the greater influence of p_5 and s_1 compared to p_2 and s_2, respectively, (Fig. 6, 7) on the proportion of the co-infected at average harvesting day (U135). One should hypothesise that p_1 will also have a weaker effect than p_5 because p_1 will also create the contrasting effect on the production of U, similar to p_2. However, the strength of the effect of p_1 and p_2 on RTD may depend on s_1 and s_2 (as the other way around was true; Appendix 4). Therefore, without the model calibration using the real data, it will be difficult to be certain about the importance of p_1, p_2, s_1 and s_2, especially because we extracted the possible ranges of these values from the models constructed from different methods [8, 9].

3. The effectiveness of roguing is context dependent.

According to roguing investigation, roguing can increase the yield significantly if it happened frequently enough when there was no cost related to roguing (Fig. 11A). The ratio between cost of roguing per individual rice hill per the net profit from one yielding host (**Cr/Pr**) varies depending on areas and varieties of rice but mostly between 0-20 [22], so the most-cost effective inter-rogue gaps were either 0.5-1.0 month (Fig. 11B) with a low sensitivity to the error associated with yield coefficient of the most yield contributing compartment (Z135) (Fig. 12). This contrasted with the conclusion from HC1996 [8] stating that roguing was impractical for RTD as it was effective only 1) when there was a low incidence or 2) when the transmission rate or vector numbers was low and the reduction in transmission as the source plants age was strong. Partially, this may be because they simulated discontinuous roguing (weekly; 4 times), so more RTD cases could undisturbedly develop during unrouged period compared to our continuous roguing consideration.

4. Further adaptation of the stochastic model

4.1. Acknowledging latent and incubation period.

The mean 6.25-day difference between RTD latent and incubation period where an inoculated host can be an effective source of virus but does not show the symptoms (cryptic infection) can have consequence on the outcome of models. Especially because the symptoms may significantly deter vectors, e.g. by the altered phenolic level or leaf colour changes [5, 23], resulting in the decreased transmission rate of RTBV or RTSV from U ($\mathbf{s_1}$ and $\mathbf{s_2}$ < 1, [6, 9]). The deterrent effect may be so significant that even RTBV being a dependent virus on RTSV [5], there is the negative synergism between RTBV and RTSV (together they produce more severe symptoms or increased titres of one or both viruses but the transmission rates of one or both

viruses are somehow reduced). For the cryptic individuals, these deterrent effects will not occur, allowing the initial rapid spread before the onset of the symptoms (s_1 and s_2 may be more than 1 for a brief period at the beginning), potentially changing the RTD dynamics. More importantly, HC1996 has suggested that the presence of this cryptic period was an underlying reason why the roguing failed in their investigation.

4.2. Adding vector (GLH) dynamics

In general, one major factor that can influence the disease is the dynamics of vector [24]. For RTD, the main contribution is through the immigration of green leafhopper (GLH) from near-by paddy fields or other hosts. One paper [7] suggested that primary spread by RTD-infective GLH immigrants greatly affected disease progression even more than secondary spread as once they arrived the field, the overall transmission rate rapidly increased. This also quickly made roguing ineffective [7]. GLH can contribute to transgenerational disease spread as they can live in regenerated growth from rice stubbles, as well as in other hosts e.g. weeds [5] and their flying distance can be as high as 2 km [25]. Therefore, in a larger longer cultivation, adopting seasonal distance-dependent transmission rate by considering the flight pattern of GLH can help refine the model, especially if GLH transmit the viruses in semi-persistent manner (GLH loses RTBV and RTSV in 4 and 7 days, respectively [5]) and environment can affect GLH growth more than rice [14].

Conclusion

Our analysis can show the that stochastic modelling may not be necessary for a multiple-pathogenic disease, caused by a synergistic relationship between pathogens, such as Rice Tungro Disease (RTD), and that parameter space exploration can be used to study the effect of parameters on RTD progression and search for conditions with high RTD incidence without prior biological knowledge. An error-insensitive index for the cost effectiveness of

roguing control can be formed and used to find the optimum pattern of roguing for RTD. However, there exists the opportunities for increasing the complexity of the models to better represent the biology of the disease and resolve the conflict on roguing effectiveness with previous literature.

Acknowledgement

I would like to thank Nik Cunniffe and Rachel Murry-Watson for providing me useful resources for stochastic modelling, helping with coding and data interpretation and presentation.

References

[1] A. Ficke, C. Cowger, G. Bergstrom, and G. Brodal, 'Understanding Yield Loss and Pathogen Biology to Improve Disease Management: Septoria Nodorum Blotch - A Case Study in Wheat', *Plant Disease*, vol. 102, no. 4, pp. 696–707, 2018, doi: 10.1094/PDIS-09-17-1375-FE.

[2] T. C. B. Chancellor, Ed., *Rice tungro disease management: proceedings of the International Workshop on Tungro Disease Management, Los Baños, Philippines*. Makati City: IRRI, 1999.

[3] P. Tennant, A. Gubba, M. Roye, and G. Fermin, 'Viruses as Pathogens', in *Viruses*, Elsevier, pp. 135–156, 2018. doi: 10.1016/B978-0-12-811257-1.00006-1.

[4] J. Ali and S. H. Wani, Eds., *Rice Improvement: Physiological, Molecular Breeding and Genetic Perspectives*. Cham: Springer International Publishing, 2021. doi: 10.1007/978-3-030-66530-2.

[5] O. Azzam and T. C. B. Chancellor, 'The Biology, Epidemiology, and Management of Rice Tungro Disease in Asia', *Plant Disease*, vol. 86, no. 2, pp. 88–100, 2002, doi: 10.1094/PDIS.2002.86.2.88.

[6] J. Holt and T. C. B. Chancellor, 'Simulation Modelling of the Spread of Rice Tungro Virus Disease: The Potential for Management by Roguing', *The Journal of Applied Ecology*, vol. 33, no. 5, pp. 927, 1996, doi: 10.2307/2404674.

[7] T. C. B. Chancellor, Ed., *Epidemiology and management of rice tungro disease: the outcome of the Rice Tungro Management Workshop 11-14 November 1993, Alor Setar, Malaysia*. Chatham, Maritime, Kent: Natural Resources Institute, 1997.

[8] J. Holt and T. C. B. Chancellor, 'Simulation Modelling of the Spread of Rice Tungro Virus Disease: The Potential for Management by Roguing', *The Journal of Applied Ecology*, vol. 33, no. 5, pp. 927, 1996, doi: 10.2307/2404674.

[9] N. Blas and G. David, 'Dynamical roguing model for controlling the spread of tungro virus via *Nephotettix Virescens* in a rice field', *J. Phys.: Conf. Ser.*, vol. 893, pp. 012018, 2017, doi: 10.1088/1742-6596/893/1/012018.

[10] N. J. Cunniffe, F. F. Laranjeira, F. M. Neri, R. E. DeSimone, and C. A. Gilligan, 'Cost-Effective Control of Plant Disease When Epidemiological Knowledge Is Incomplete: Modelling Bahia Bark Scaling of Citrus', *PLoS Comput Biol*, vol. 10, no. 8, pp. e1003753, 2014, doi: 10.1371/journal.pcbi.1003753.

[11] H. Andersson and T. Britton, *Stochastic epidemic models and their statistical analysis*. New York: Springer, 2000.

[12] M. J. Keeling and J. V. Ross, 'On methods for studying stochastic disease dynamics', *J. R. Soc. Interface.*, vol. 5, no. 19, pp. 171–181, 2008, doi: 10.1098/rsif.2007.1106.

[13] M. J. Keeling and P. Rohani, *Modeling infectious diseases in humans and animals*. Princeton: Princeton University Press, 2008.

[14] K.-H. Kim, A. D. Raymundo, and C. M. Aikins, 'Development of a rice tungro epidemiological model for seasonal disease risk management in the Philippines', *European Journal of Agronomy*, vol. 109, pp. 125911, 2019, doi: 10.1016/j.eja.2019.04.006.

[15] D. T. Gillespie, 'A general method for numerically simulating the stochastic time evolution of coupled chemical reactions', *Journal of Computational Physics*, vol. 22, no. 4, pp. 403–434, 1976, doi: 10.1016/0021-9991(76)90041-3.

[16] X.-S. Zhang, J. Holt, and J. Colvin, 'Synergism between plant viruses: a mathematical analysis of the epidemiological implications: Synergism between plant viruses', *Plant Pathology*, vol. 50, no. 6, pp. 732–746, 2001, doi: 10.1046/j.1365-3059.2001.00613.x.

[17] P. Reuben *et al.*, 'Optimizing Plant Spacing under the Systems of Rice Intensification (SRI)', *AS*, vol. 07, no. 04, pp. 270–278, 2016, doi: 10.4236/as.2016.74026.

[18] Y. Singh *et al.*, 'Direct Seeding of Rice and Weed Management in the Irrigated Rice- Wheat Cropping System of the Indo-Gangetic Plains', *Los Baños, Philippines*. Makati City: IRRI, 2008.

[19] H. Hibino, H. Leung, and Teng, P.S., 'YIELD LOSS DUE TO RICE VIRUS DISEASES IN ASIAN TROPICS', *jircas*, vol. 22, pp. 93–100, 1988.

[20] H. Zhang and T. Zhang, 'Dynamics Analysis of a Stochastic Plant Disease Model with Continuous Cultural Control Strategy', *Complexity*, vol. 2021, pp. 1–15, 2021, doi: 10.1155/2021/5550131.

[21] C. A. Gilligan, 'An epidemiological framework for disease management', in *Advances in Botanical Research*, Elsevier, vol. 38, pp. 1–64, 2002. doi: 10.1016/S0065-2296(02)38027-3.

[22] Faculty of Business Administration, Huachiew Chalermprakiet University, Cost and Return on Rice RD15 Farming by the Farmers in Pong Srinakron Village, Rong Chang Sub-district, Pa Daet District, Chiang Rai Province, Business Review, vol. 10, no. 1, pp. 7-23, 2018

[23] G. Kumar and I. Dasgupta, 'Comprehensive molecular insights into the stress response dynamics of rice (Oryza sativa L.) during rice tungro disease by RNA-seq-based comparative whole transcriptome analysis', *J Biosci*, vol. 45, no. 1, pp. 27, 2020, doi: 10.1007/s12038-020-9996-x.

[24] J. K. Brown, Ed., *Vector-mediated transmission of plant pathogens*. St. Paul, Minnesota: APS Press, 2016.

[25] T. C. B. Chancellor, J. Holt, S. Villareal, E. R. Tiongco, and J. Venn, 'Spread of Plant Virus Disease to New Plantings: A Case Study of Rice Tungro Disease', in *Advances in Virus Research*, Elsevier, vol. 66, pp. 1–29, 2006. doi: 10.1016/S0065-3527(06)66001-6.

Supplementary Figure

Supplementary Figure 1.1 and 1.2: Progress curve of Rice Tungro Disease (RTD) from stochastic runs examining the effect of p_2

1.1

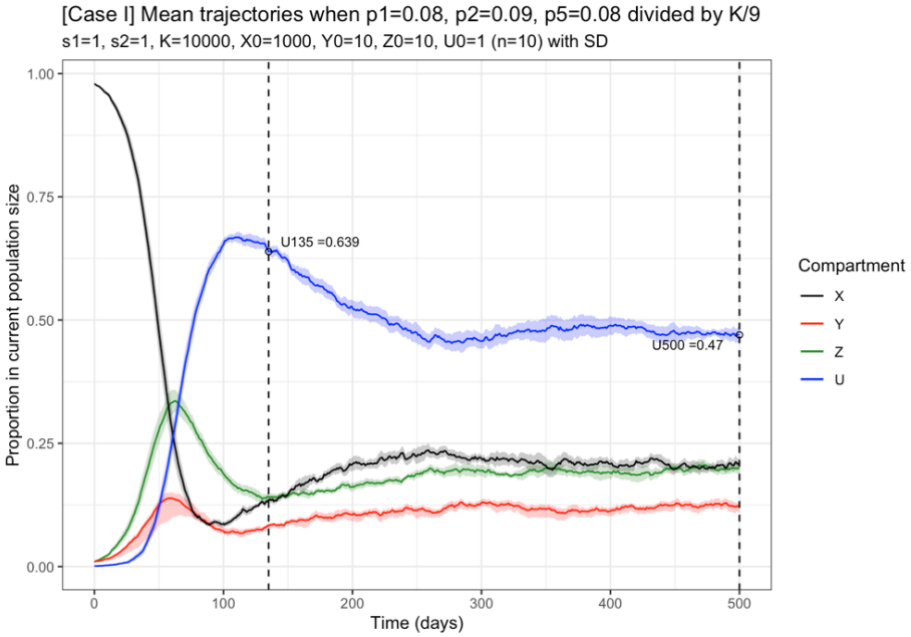

1.2

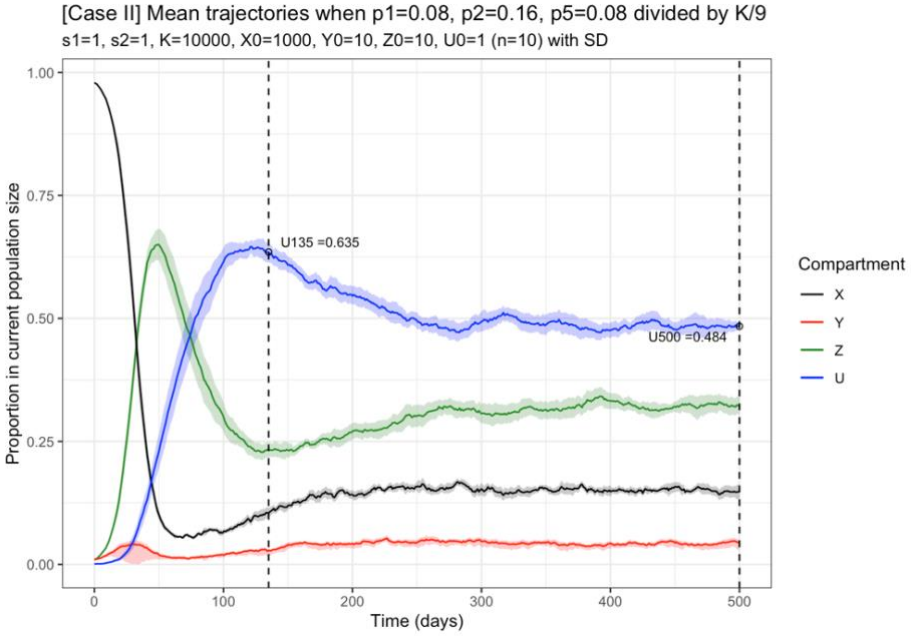

The mean proportions of each host compartments: the susceptible (X), the RTBV-infected (Y), the RTSV-infected (Z) and the co-infected (U), colour-coded as in the legend, from 10 simulations were plotted with SD (shaded areas). The transmission-related parameters and initial conditions used are stated in the titles; the only difference was p_2: Case I used p_2= 0.09/(K/9) based on HC1996 paper, lower than p_2= 0.16/(K/9) based on BD2017 paper in Case II. They had similar U trajectories, although Z hit a higher peak in Case II.

Supplementary Figure 2.1 and 2.2: Progress curve of RTD dynamics from stochastic runs examining the effect of p_5

2.1

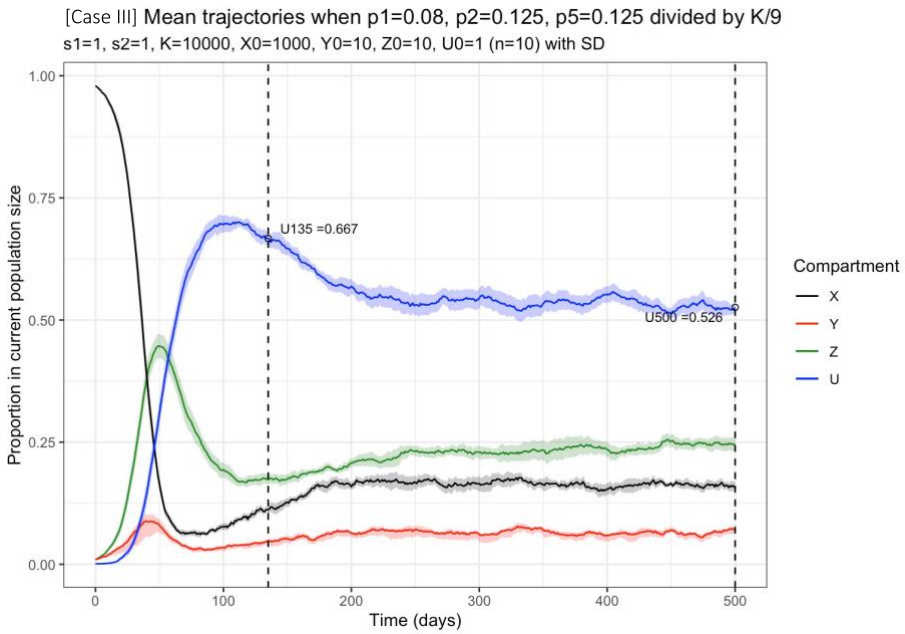

2.2

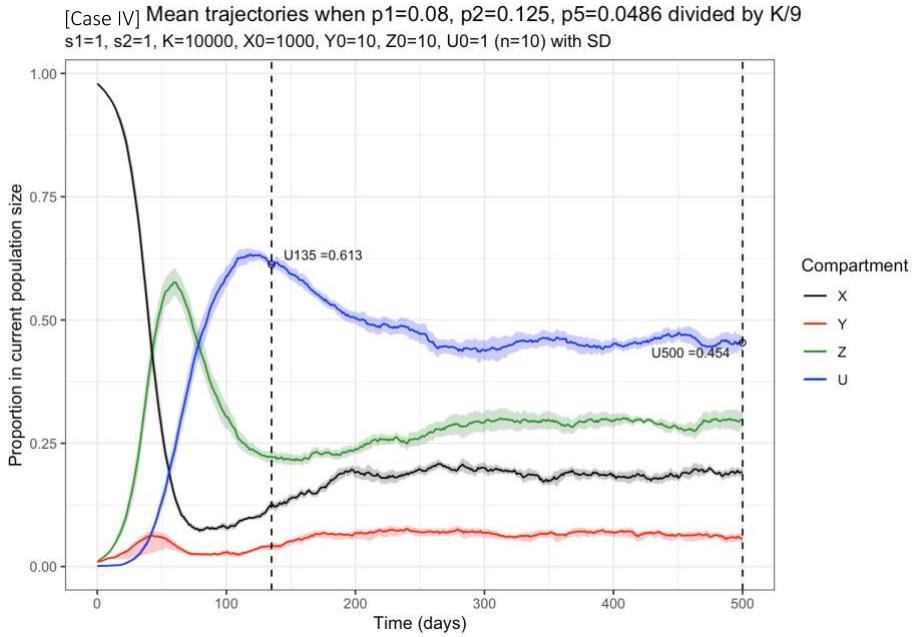

The mean proportions of each host compartments: the susceptible (X), the RTBV-infected (Y), the RTSV-infected (Z) and the co-infected (U), colour-coded as in the legend, from 10 simulations were plotted with SD (shaded areas). The transmission-related parameters and initial conditions used are stated in the titles; the only difference was p_5: Case III used p_5 = 0.125/(K/9) based on HC1996 paper, lower than p_5= 0.0486/(K/9) based on BD2017 paper in Case IV. They had similar U trajectories, as well as other compartments.

Supplementary Figure 3.1 and 3.2: The two-way s_1-s_2 scan outcome of the co-infected (U) at day 135 that can show the negative relationship between RTBV and RTSV.

3.1

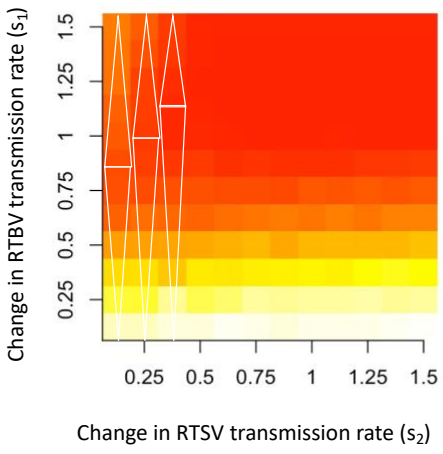

3.2

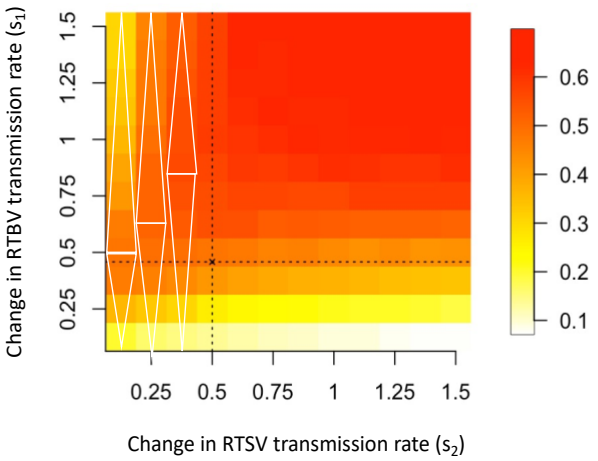

s_1 is the change in transmission rate of RTBV due to a source previously being infected by RTSV and ***s_2*** is the change in transmission rate of RTSV due to a source previously being infected by RTBV. Color represents the value of the proportion of RTD-affected host at day 135 (U135) as shown in the legend. The white triangles represent the gradient of the colour, with the base being the darkest tone and where the trend of colour change reversed. This reversal happened earlier with the lower ***s_2***. The two different initial conditions were used with the same ***p_{1d}***, ***p_{2d}***, and ***p_{5d}***: Y0=Z0=10 and U0=1 in Fig 3.1 and Y0=Z0=U0=100 in Fig. 3.2, while X0=1000 in both. Regardless of the initial conditions, when ***s_2*** was low, increasing ***s_1*** increased U135 at first, but then caused it to drop (this can potentially be seen for all ***s_2*** if we were to increase the scanning range). It may mean that there was a threshold of the RTSV level in the system, above which RTBV cannot persist.

Supplementary Figure 4.1 and 4.2: The two-way s_1-s_2 scan outcome of the RTBV-infected (Y) and the RTSV-infected (Z) at day 135, respectively.

4.1

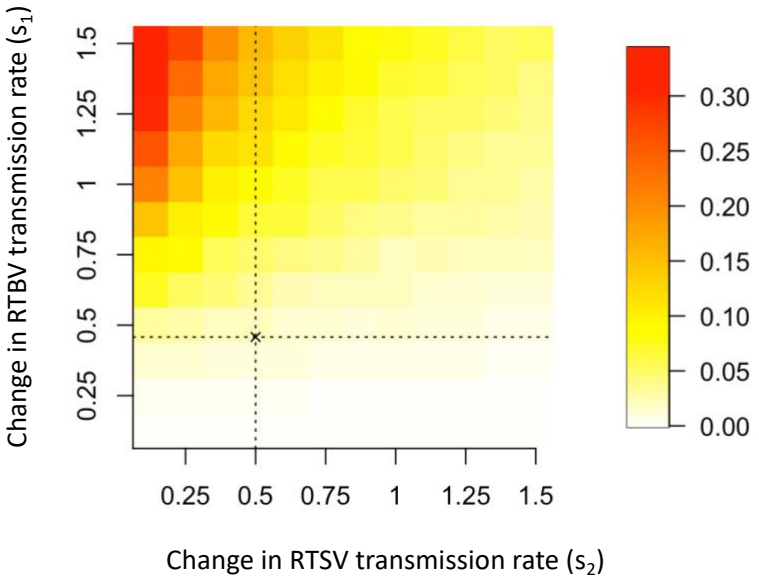

4.2

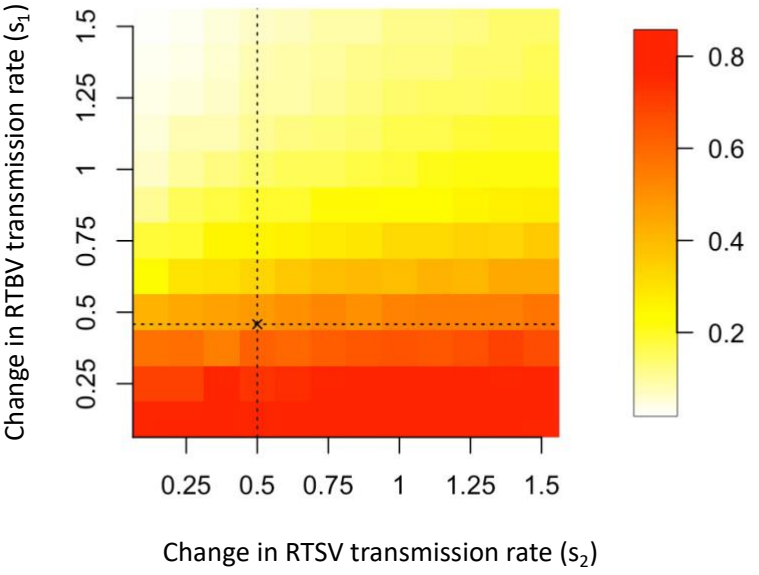

s_1 is the change in transmission rate of RTBV due to a source previously being infected by RTSV and ***s_2*** is the change in transmission rate of RTSV due to a source previously being infected by RTBV. RTBV singly infected hosts (Y) can only increase when ***s_1*** is high enough. Similarly, RTSV singly infected hosts (Z) can only increase when ***s_2*** is high enough, but with a lower threshold. Also note the difference in the color scale; Z can increase to a larger proportion than Y. In almost all cases, Z dominated Y, well-reflected by 1) its low death rate due to little to no symptoms and 2) the higher transmission rate (***p_2***) compared to RTBV transmission rate (***p_1***). A cross (×) represents U135 proportion, given by this pair ***s_1*** and ***s_2*** equal to 0.458 and 0.500, respectively.

Supplementary Figure 5.1: Examples of progress curves from rogued situations with different length of inter-rogue gaps.

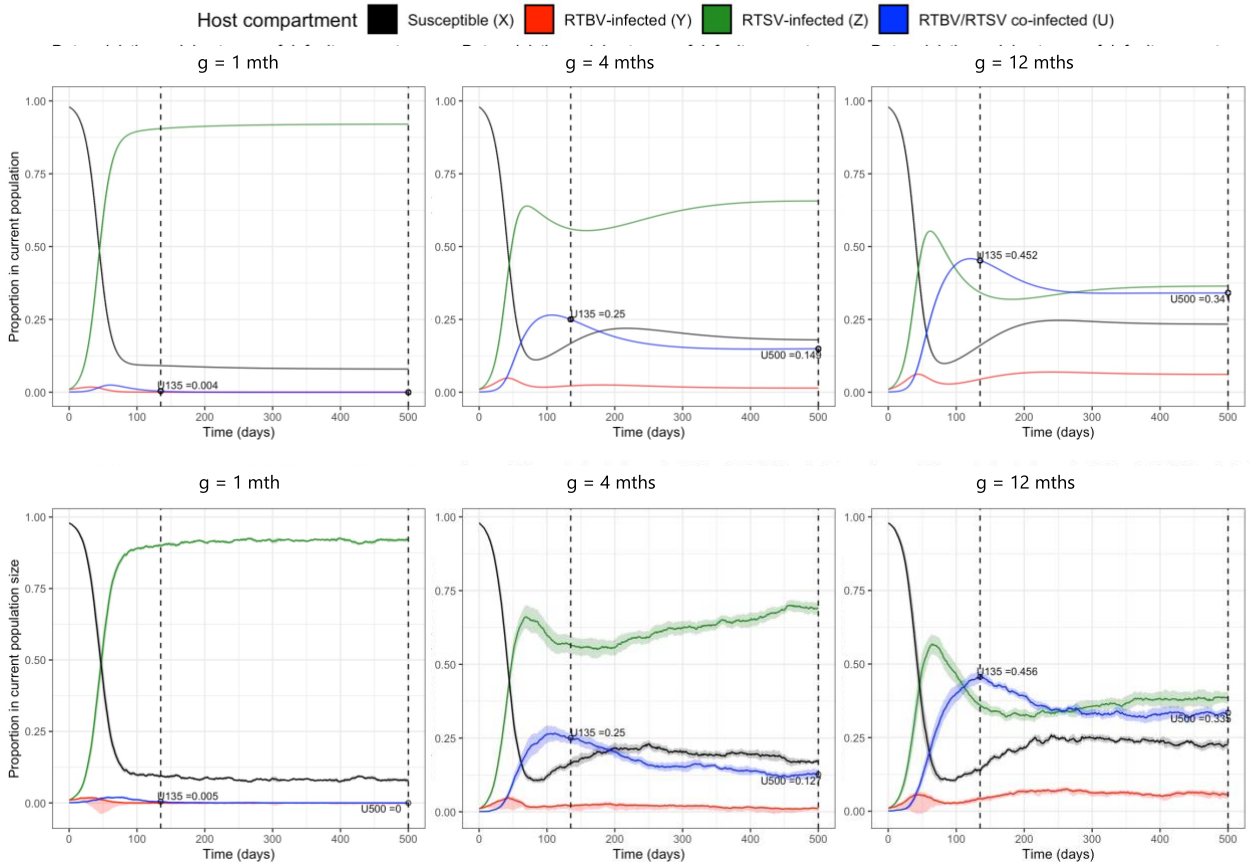

The first row was the trajectories from deterministic simulations and the second row showed the mean from 10 stochastic runs. There was no difference from both model for all gaps. Initial conditions used were X0=1000, Y0=10=Z0, U0=1. Parameters were default shown in Sup. Table 3.1 and Appendix 5. From left to right, the gap was 1, 4, and 12 months. As the gap was longer, the proportion of Z at day 135 markedly increase, U135 and Y135 decreased and X135 hovered around 0.10.

Supplementary Figure 5.2: The yield contribution of each host compartment (based on *Yd*; equation (6)).

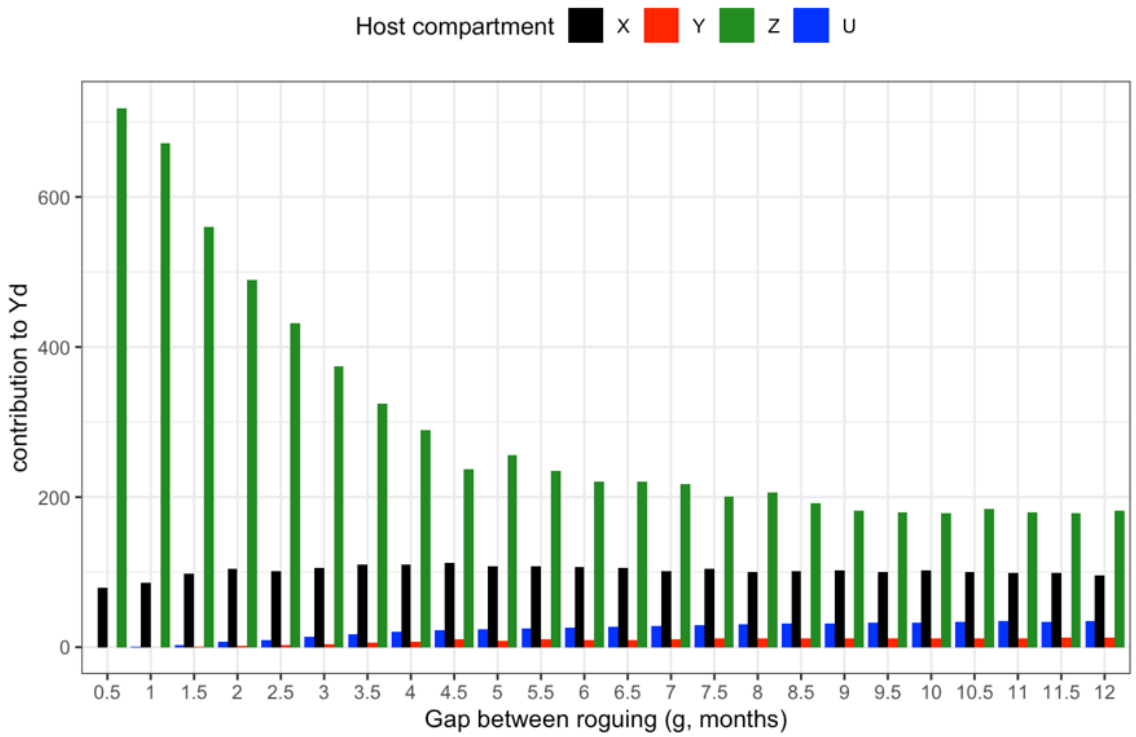

For all roguing gaps, RTSV-infected hosts (Z) contributed the most to the total yield (***Yd***) due to 1) its high abundance and 2) its high yield coefficient ($\mathbf{c_2}$ = 0.78), followed by the healthy hosts (X). The least contributing compartment was RTBV-infected hosts as it got rogued, leading to a low abundance and its low yield coefficient ($\mathbf{c_1}$ = 0.46), although this was still more than that of the co-infected (RTD-affected) hosts (U) ($\mathbf{c_3}$ = 0.12).

Supplementary Figure 6: Exemplified case of one-compartment extinction case.

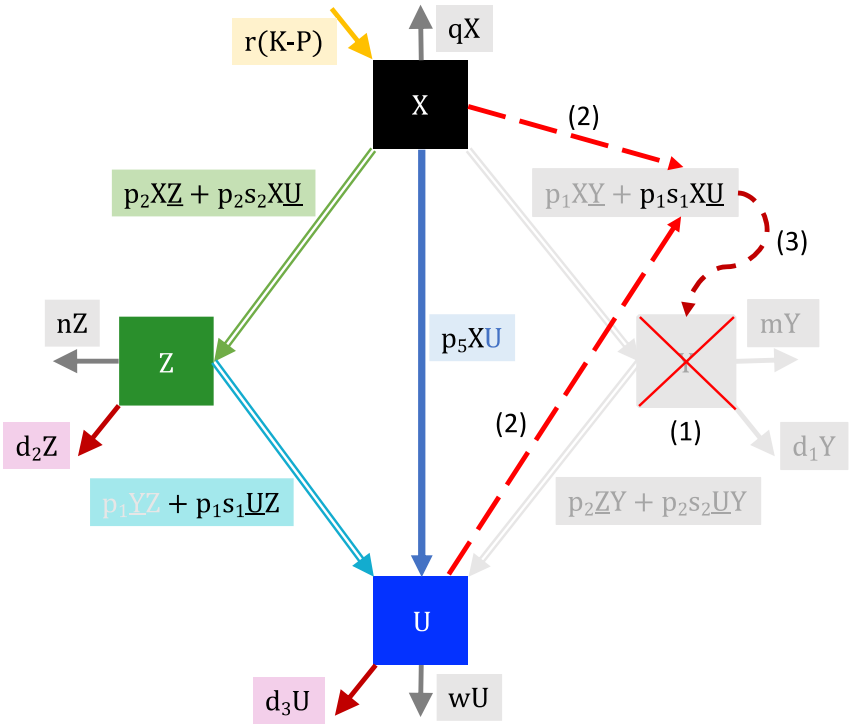

(1) RTBV-infected hosts (Y) become extinct, making to all transmission events contributed by the inoculum Y and demographic changes of Y) become non-feasible (shown by grey letters and boxes)

(2) However, non-zero susceptible hosts (X) and the co-infected (U) can contribute to one pathway that leads to the production of Y

(3) As a result, Y recovers from zero.

The likely recovery from zero of host compartments also applies to RTSV-infected (Z) and U compartments. This makes the simultaneous extinction of two or three compartments unlikely.

Supplementary Table

Supplementary Table 1: Probability of events and its consequence on the abundance of each host compartment (plants per area).

Event	Probability (Divided by T*)	Consequence**			
		X	Y	Z	U
Planting of new susceptible plant	$r(K-P)$	+1	0	0	0
Death of the susceptible	qX	-1	0	0	0
Death of the RTBV singly infected	mY	0	-1	0	0
Death of the RTSV singly infected	nZ	0	0	-1	0
Death of the RTBV/RTSV doubly infected	wU	0	0	0	-1
Transmission of RTBV into the susceptible	$p_1(Y+s_1U)X$	-1	+1	0	0
Transmission of RTSV into the susceptible	$p_2(Z+s_2U)X$	-1	0	+1	0
Co-transmission of RTBV and RTSV into the susceptible	p_5UX	-1	0	0	+1
Transmission of RTBV into the RTSV singly infected	$p_1(Y+s_1U)Z$	0	0	-1	+1
Transmission of RTSV into the RTBV singly infected	$p_2(Z+s_2U)Y$	0	-1	0	+1
Roguing of the RTBV singly infected	d_1Y	0	-1	0	0
Roguing of the RTSV singly infected	d_2Z	0	0	-1	0
Roguing of the RTBV/RTSV doubly infected	d_3U	0	0	0	-1

*Total rate (T)= $r(K-P)+p_1(Y+s_1U)X+p_2(Z+s_2U)X+p_5UX+p_2(Z+s_2U)Y+p_1(Y+s_1U)Z+qX+mY+nZ+wU+d_1Y+d_2Z+d_3U$

** Increase or decrease by 1 [plant][area]$^{-1}$ is represented by +1 or -1, respectively, and 0 means no change

Supplementary Table 2: Parameter value summary from HC1996 and BD2017 paper

Virus transmission events			**Parameters**	
Virus that infects	Transition	Source	**HC1996 paper** (t is probabilities)	**BD2017 paper** (Each to be divided by current total host abundance)
Case1: +RTBV	X to Y or Z to U	Y	t_2 = 0.08	Sigma = 0.08
Case2: +RTSV	X to Z or Y to U	Z	t_1 = 0.16	Beta = 0.09
Case3: +RTBV	X to Y or	U	t_3 = 0.02 (s_1 = 0.25)	Tau = 0.06 (s_1 = 0.75)
	Z to U			Lambda = 0.03 (s_1 = 0.375)
Case4: +RTSV	X to Z or	U	t_2 = 0.08 (s_2 = 0.5)	Gamma = 0.01 (s_2 = 0.125)
	Y to U			Delta = 0.07 (s_2 = 0.875)
Case5: +both	X to U	U	t_1 = 0.16	Alpha = 0.035
	Other events		**HC1996 paper**	**BD2017 paper**
Host planting rate			-	r = 0.001
Maximum host abundance when birth rate is zero			-	P_0 = 20000
Death rate of X			-	q_0 = 0.008
Death rate of Y			-	q_1 = 0.009
Death rate of Z			-	q_2 = 0.0125
Death rate of U			-	q_3 = 0.025
Roguing efficiency for Y, Z, and U, respectively			0.7, 0.0, 1.0	-

*Note that mean value of s_1 = 0.458 and s_2 = 0.500

Supplementary Table 3.1: Fixed values of parameters used for comparative runs (Method 1.3; excluding *) and parameterisation (Method 2; including *)

Events or Constants	Parameter	Value
Host planting rate	r	0.001
Maximum host abundance when birth rate is zero	K	10000
Death rate of X	q	0.0080
Death rate of Y	m	0.0125
Death rate of Z	n	0.0090
Death rate of U	w	0.0250
*(RTBV transmission from RTBV-singly infected host (Y))	(p_1)	(0.008/(K/9))

Supplementary Table 3.2: Ranges of non-fixed parameters for comparative runs

Events or Constants	Parameter	Range
• RTBV transmission from RTBV-singly infected host (Y) • RTSV transmission from RTSV-singly infected host (Z) • Co-transmission of RTBV and RTSV from RTBV/RTSV-doubly infected (U)	p_1 p_2 p_5	0.08/(K/9) – 0.16/(K/9)
• Change in transmission rate of RTBV due to a source previously being infected by RTSV • Change in transmission rate of RTSV due to a source previously being infected by RTBV	s_1 s_2	0.125-2.00

Supplementary Table 3.3: Six sets of initial conditions used for comparative runs

Initial Condition Set ID	X0	Y0	Z0	U0
1	1000	1	1	0
2	1000	100	200	0
3	1000	200	100	0
4	1000	100	100	100
5	7500	100	100	100
6	7500	500	500	500

Supplementary Table 3.4: The "extreme" parameter set that produced all-host out-of-range ratios (more than 1.5 or less than 0.5).

p_1	p_2	p_5	s_1	s_2
0.09/(K/9)	0.13/(K/9)	0.16/(K/9)	1.7	0.7
initial set	**X0**	**Y0**	**Z0**	**U0**
1	1000	1	1	0

Supplementary Table 4: Host abundances at day 135 and index ***Yd*** (equation (6)) in the unrouged situation with the default parameters shown Appendix 4 (Table B)

Model	**Host Abundances**				**Total Abundance**	Index
	X135	Y135	Z135	U135	(P135)	***Yd***
Deterministic	112	52	97	307	568	248
Stochastic	121	49	94	294	558	252

The numbers are rounded to an integer. The units are plants per area

Appendix

Appendix 1: Construction of the death rate due to roguing (d_i)

The probability of detection (e_i) of different infected compartments were assigned based on Holt & Chancellor (1996) (Sup. Table 1). We were interested in the effect of duration between roguing operation (g) on the yield. The roguing-related death rate (d_i) took into account both parameters.

The death rate of each infected host due to roguing (d_i) is the reciprocal of the average effective infectious period of that host which depends on roguing gap (g). The effective infectious period is equal to the duration between the round of rouging before the plant becomes infectious/symptomatic and the round that the host gets rogued on average (duration A) subtracted by the duration between the final round of rouging and the emergence of infectivity/symptom (duration B).

Duration A is equal to the gap if the probability of detection (e) is 1.0 (no host can escape the roguing), but it gets longer than the gap as the probability decreases. The increase in the duration is by the factor of $1/e$ as the number of roguing rounds required for detecting hosts after it becomes infectious/symptomatic is also increased by this factor (when it is assumed to be geometric random variable, with the average $1/e$). For example, if 50% infected hosts get detected at each roguing ($e = 0.5$), on average, it will take 2 rounds (1/0.5) of roguing to detect and rogue these hosts, meaning the duration A is also doubled ($g/e = g/0.5$). In our model, we ignored the consideration of the latent and incubation period, so the emergence of infectivity and symptoms were virtually at the same time (when the virus(es) got inoculated onto the host).

Duration B, on average, is the half of the gap length ($g/2$) when we assume the uniform distribution of the transition from X to U (or to Z) between rounds of roguing for each roguing gap (g). This requires us to ignore the potential change in the rates of the transition due to the change in the abundance of each host compartment between rounds of roguing. In other words,

we assume that X can become U (or to Z) at any time point with the identical probability within the gap and as time passes. Therefore, we obtained equation (5) as follow:

$$\text{Death rate due to roguing } (\boldsymbol{d_i}) = \frac{1}{\text{Effective infectious period}} = \frac{1}{\text{Duration A - Duration B}} = \frac{1}{\frac{\boldsymbol{g}}{\boldsymbol{e_i}} - \frac{\boldsymbol{g}}{2}}$$

Appendix 2: Normalisation of p_1 and the other transmission rates

Holt & Chancellor (1996, [8]) and Blas & David (2017, [9]) both considered plant and vector dynamics in their model. The variable representing the transmission of RTBV from RTBV singly infected (Y) was in the probability form in HC1996 (t_2 = 0.08). In BD2017, the equivalent was sigma (sigma = 0.08), but transmission terms in their ODEs were divided by the total current population. Since our model did not considered vector dynamics, represented each compartment in the number, not proportion, (Fig. 1) and used the rates, not probability, to factor with each term in ODEs, we then need to change the absolute values 0.08 that they used in the models by dividing 0.08 by f(***K***), where ***K*** is the maximum number of hosts when the birth rate is zero ($\boldsymbol{r(K-P) = 0}$).

To obtain a reasonably large population at steady state, f(***K***) was determined based on the steady state value of the susceptible hosts ($\frac{\boldsymbol{dX}}{\boldsymbol{dt}} = \boldsymbol{0}$), when there is no disease ($\boldsymbol{Y = U = Z = 0}$, so $\boldsymbol{P = X + Y + Z + U = X}$), which can be obtained as below:

$$\frac{dX}{dt} = r(K-P) - p_1(Y + s_1U)X - p_2(Z + s_2U)X - p_5UX - qX = 0$$

$$\frac{dX}{dt} = r(K-X) - qX = 0$$

$$rK - rX - qX = 0$$

$$X = \frac{rK}{r+q}$$

This means that the disease-free steady state number of X depends on the values of ***r***, ***K*** and ***q***, and it equals to ***K***/9 as we set ***r*** = 0.001 and ***q*** = 0.008 (Sup. Table 1); therefore, f(***K***) should be equal to ***K***/9. With this decision, the size of $\boldsymbol{p_1}$ was only reduced by the size of small long-term population (carrying capacity when birth and death rate are not zero). If we were to use ***K*** as a

denominator, we would obtain too low incidence of RTD due to excessively reduced transmission rates, which is what can be seen from BD2017. This would not be suitable for further investigation of roguing effect.

Appendix 3.1: Calculation of roguing distance for our model

One rice hill (one plant in our investigation) is usually allowed to occupy 25x25 cm^2 area of land (the space between the hill is 25 cm in all directions) [6], and therefore, the maximum host capacity (***K***) of 10,000 host plants used in our model represents a square rice paddy with 2500x2500 cm^2 or 25x25 m^2 area (or 625 m^2). For roguing operation, assuming walking along one line in the middle between two rows of rice allows the inspection of both rows, the staff only need to walk a 25.5-m distance to survey 2 rows, which amount to 50 times overall for 100 rows (Figure A). Therefore, they need to walk which equal to 1275 m or 1.28 km. Therefore, little human resource is needed, especially considering the fact that the host abundance was usually much lower than 10,000 in our model; a large portion of the paddy will not need the survey. However, a larger labour requirement will be applied for a larger-scale rice paddy.

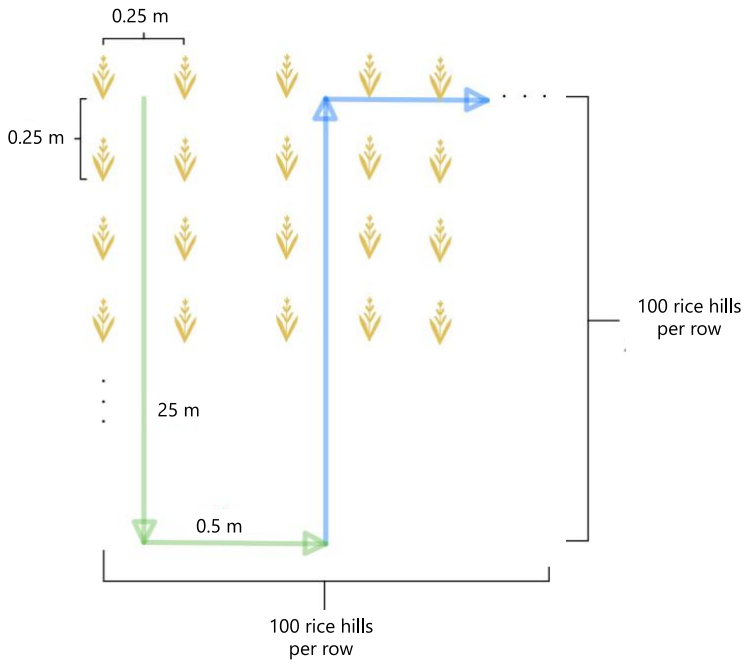

Figure A: The 25.5m-long green path was drawn for the roguing survey of the first 2 rows of rice hills (100 hills per row, so each row is 0.25x100 = 25 m long). The blue path represented the survey distance of the second 2 rows. To complete the survey of a paddy with 100x100 (10,000) rice hills is, therefore, 25.5m x 50 = 1275 m.

Appendix 3.2: Infection age-dependent yield losses

Yield losses due to the infection of either or both RTBV and RTSV decreases as rice hosts get infected later after planting. Generally, the number of tillers (shoots that arise from the base of a grass plant) determined the yield , and it is negatively affected if rices reduce nutrients [7], which can be due to poor root development, induced by the infection of one of these viruses (with the most severe being due to the co-infection). Infected at the early stage from germination to tillering stage (vegetative phase), which lasts 45-55 days for Taichuang 1 (TN1) that are short-duration variety [7], the disease then can reduce the yield much more than infection in the later stage (from panicle initiation and to flowering phase).

The percentage yield loss of TN1 (Taichuang 1) varieties due to RTBV, RTSV, or co-infection [8] and calculated yield coefficients is shown in the **Table A** below:

Infection time (days after planting)	Yield loss		
	RTBV (Y)	RTSV (Z)	Both (U)
7	83	27	95
21	70	22	94
35	35	20	90
49	28	20	75
Average yield loss	54	22	88
Average yield	46	78	12
Yield coefficient	c_1 = 0.46	c_2 = 0.78	c_3 = 0.12

Note that since the yield reduction of RTBV/RTSV co-infected plants was reduced to only 5% if plants get infected at 60 days after planting [], we then disregard yield losses after 49 days, at which information can be found for all types of infection.

Appendix 4: The strength of the influence of the change in transmisiion rate of each virus due to a source having the other virus on the U135 proportion.

$\mathbf{s_1}$ is change in transmission rate of RTBV due to a source previously being infected by RTSV) **and** $\mathbf{s_2}$ is change in transmission rate of RTSV due to a source previously being infected by RTBV

$\mathbf{p_1}$ is the transmission rate of RTBV from the RTBV-singly infected (Y) and $\mathbf{p_2}$ is the transmission rate of RTSV from the RTSV-singly infected (Z), set at 0.08/(K/9) and 0.125/(K/9), respectively in the normal two-way $\boldsymbol{s_1}$-$\boldsymbol{s_2}$ scan (Fig. 7). The scan outcome with the swapped values of $\mathbf{p_1}$ and $\mathbf{p_2}$ switched the pattern seen in the normal scan (i.e. transpose the color matrix) (Fig. H). In contrast, when the death rates of Y and Z were swapped, there were no change in the colour pattern (not shown), further supporting that the depend on the relative values of $\mathbf{p_1}$ and $\mathbf{p_2}$ of the relative influence strength of $\mathbf{s_1}$ and $\mathbf{s_2}$

Fig. H

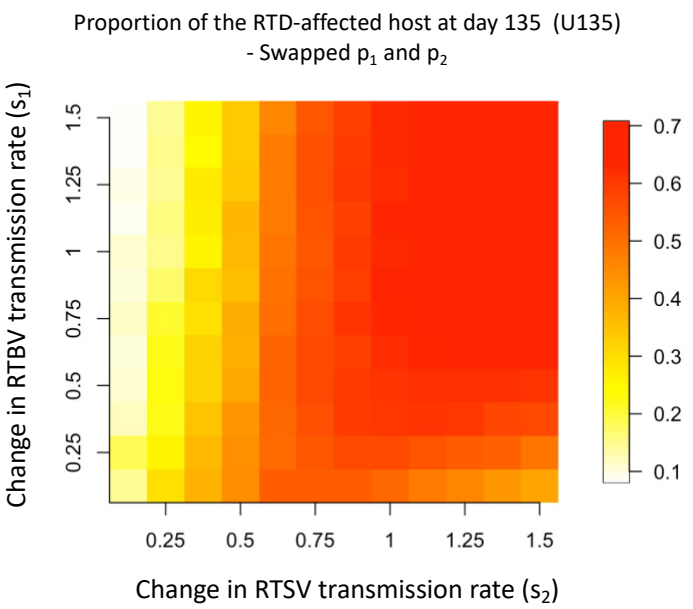

VS

Fig. 7
Normal scan

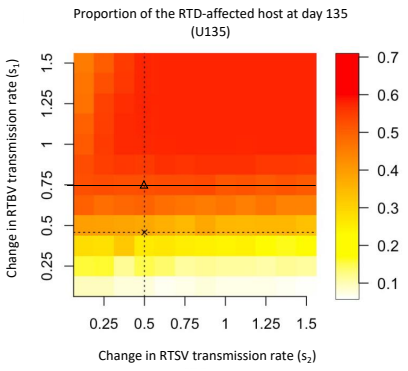

Figure H: two-way $\boldsymbol{s_1}$-$\boldsymbol{s_2}$ scan outcome using the transmission rate of RTBV ($\mathbf{p_1}$) and the transmission rate of RTSV ($\mathbf{p_2}$) equal to 0.125/(K/9) and 0.08/(K/9), respectively. The horizontal gradients were steeper than the vertical ones, reflecting the greater influence of $\mathbf{s_1}$ on U135 proportion compared to that of $\mathbf{s_2}$, giving the opposite conclusion to the normal scan (Fig. 7)

Appendix 5: Default values of transmission-related parameters to be used for roguing investigation. Shown in the Table B below were the values that gave high incidence of RTD at day 135 and were in the ranges cited by HC1996 and BD2017 paper. They were used with fixed parameters (Sup. table 3.1) for roguing investigation.

Virus transmission event	Transition	Source	Parameter	Default values
+RTBV	X to Y or Z to U	Y	p_1	0.080/(***K***/9)
+RTSV	X to Z or Y to U	Z	p_2	0.125/(***K***/9)
+RTBV and RTSV	X to U	U	p_5	0.086/(***K***/9)
Change in transmission rate				
Change in the transmission rate of RTBV from U compared to from Y			s_1	0.750
Change in the transmission rate of RTSV from U compared to from Z			s_2	0.500

Similar to other parameter sets, the RTD dynamics with this parameter set was only subject to demographic stochasticity when either Y0 or Z0, or both were 1 (Figure B-D). Therefore, we kept the initial condition X0=1000, Y0=10=Z0, and U0=1 as the initial condition for further roguing investigation (Fig. 9).

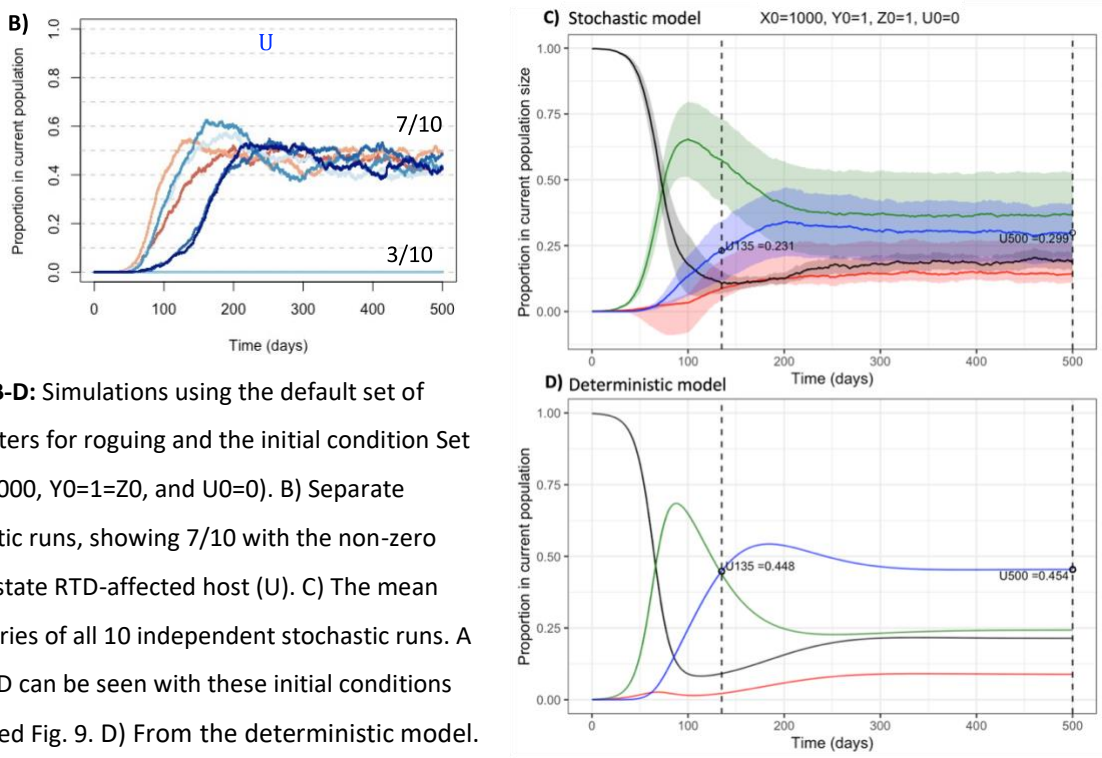

Figure B-D: Simulations using the default set of parameters for roguing and the initial condition Set 1 (X0=1000, Y0=1=Z0, and U0=0). B) Separate stochastic runs, showing 7/10 with the non-zero steady-state RTD-affected host (U). C) The mean trajectories of all 10 independent stochastic runs. A larger SD can be seen with these initial conditions compared Fig. 9. D) From the deterministic model. U135 and U500 were higher than from stochastic runs due to the non-existence of the case with the extinction of U.

Appendix 6: Progression curve from stochastic simulations using the "extreme" set of parameters (Sup. Table 3.4) but varied initial conditions.

Since X0 (the initial susceptible) and U0 (the initial co-infected) has no effects on stochasticity, in this investigation, they were kept at 1000 and 0, respectively, while Y0 (the initial RTBV-infected) and Z0 (the initial RTSV-infected) were varied to search for the minimum number of initial Y and Z that allow the resistance to demographic stochasticity. The result showed that if either Y0 or Z0 was more than 1 (Fig. G), all 10 stochastic runs followed the same trajectories. If one of them started off with 1 (Fig. E, F), the trajectories diverged, and some extinction occurred. As expected, if Z0>Y0, the extinction, if ever occurred, happened with Y (Fig. E) and Z persisted, and vice versa (Fig. F).

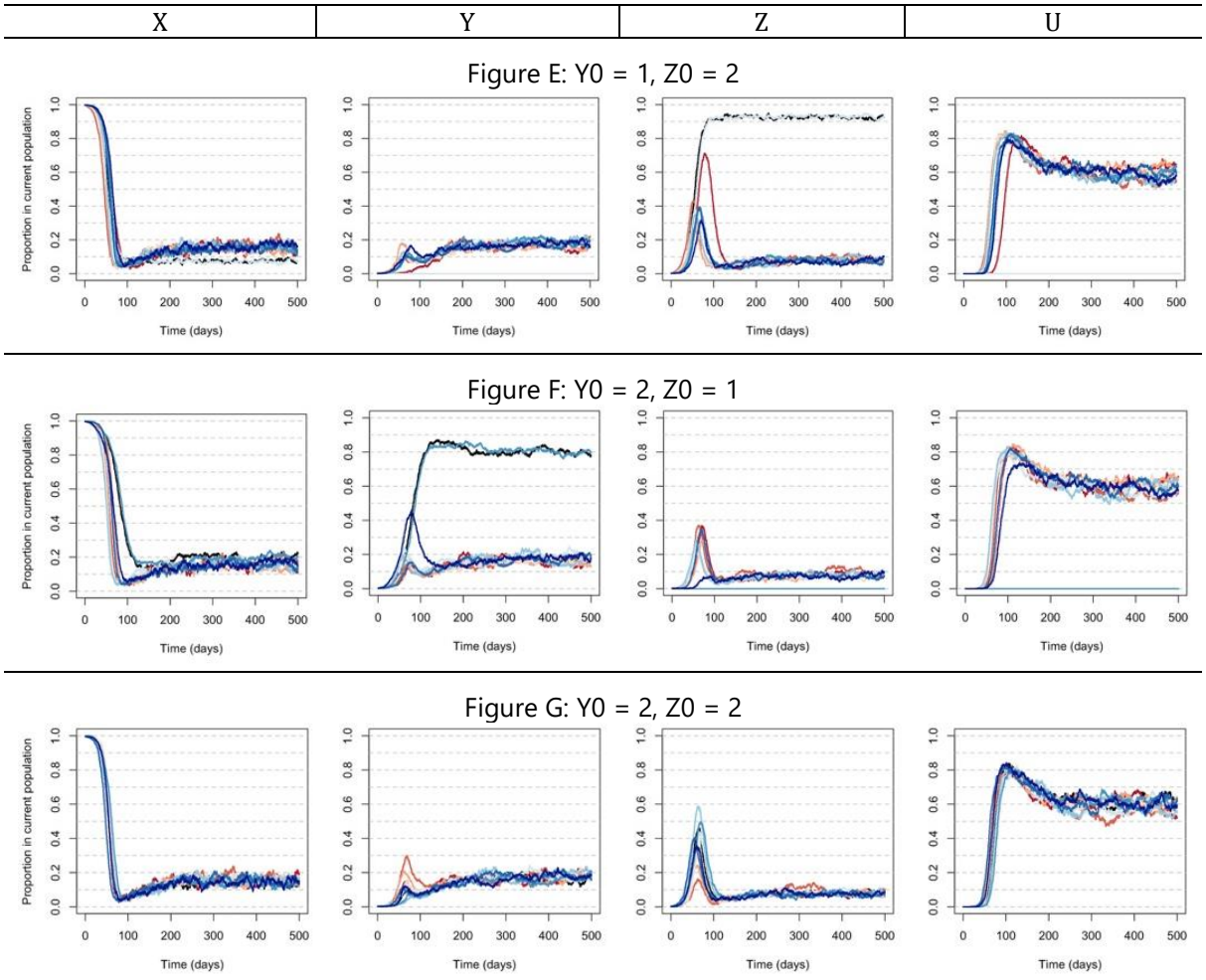

Figure E-G: the separate trajectories form 10 independent stochastic runs using $\mathbf{p_1}, \mathbf{p_2}, \mathbf{p_5}, \mathbf{s_1}, \mathbf{s_2}$ = 0.09/(K/9), 0.13/(K/9), 0.16/(K/9), 1.7, 0.7, respectively. X0=1000 and U0=0 in all cases, Y0 and zz0 varied as in the title.

Appendix 7: Lengthening the inter-rogue gaps initially increase the proportion of susceptible host (X) at day 135 (harvesting day), regardless of the initial conditions. The increase in X also does not result from the disproportionate decrease in X compared to the decrease in overall population. The abundance of X at day 135 were genuinely increased.

Figure I: X0,Y0,Z0,U0 = 1000,100,100,1

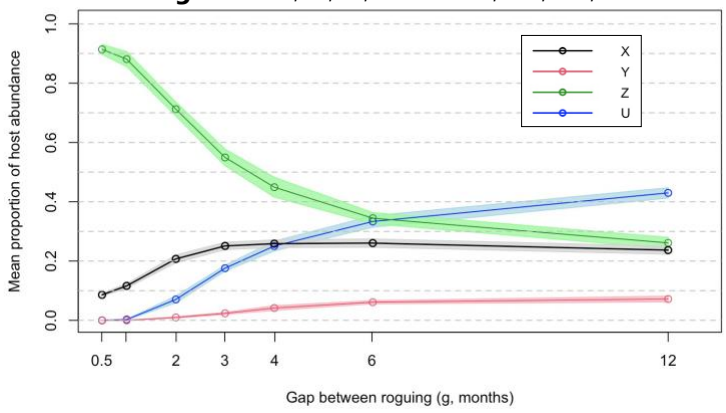

Figure I: The mean proportion of each host compartment at day 135. The initial conditions shown at the top of the graph. X135 proportion increases when the gap was increased from 0.5 to 3 months, similar to the initial condition that had much lower Y0 and Z0 (10 each) used in the main investigation. The increase was independent of Y0 and Z0.

Figure J: X0,Y0,Z0,U0 = 5000,500,500,500

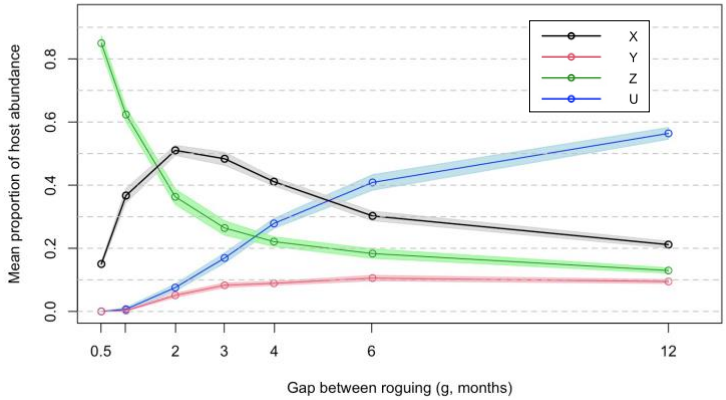

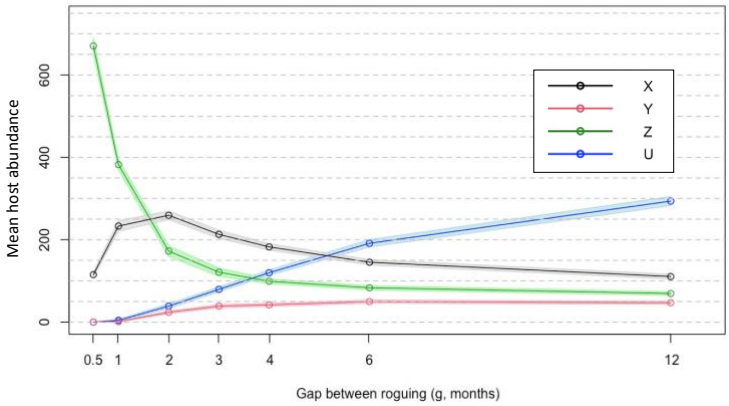

Figure J: The initial conditions shown at the top of the two graphs. The graph above shows the mean proportion of each host compartment at day 135. X135 proportion increased when the gap was increased from 0.5 to 2 months, similar to the initial condition that had much lower Y0 and Z0 (10 each) used in the main investigation. The increase was also independent of X0 and U0. The graph below shows the mean number of each host compartment at day 135. X135 number increased when the gap was increased from 0.5 to 2 month, similar to its mean proportion.